PRESSURE TRANSIENT TEST ANALYSIS OF VUGGY NATURALLY FRACTURED CARBONATE RESERVOIR: FIELD CASE STUDY

A Thesis

by

BABATUNDE TOLULOPE AJAYI

Submitted to the Office of Graduate Studies of
Texas A&M University
in partial fulfillment of the requirements for the degree of

MASTER OF SCIENCE

August 2007

Major Subject: Petroleum Engineering

PRESSURE TRANSIENT TEST ANALYSIS OF VUGGY NATURALLY FRACTURED CARBONATE RESERVOIR: FIELD CASE STUDY

A Thesis

by

BABATUNDE TOLULOPE AJAYI

Submitted to the Office of Graduate Studies of
Texas A&M University
in partial fulfillment of the requirements for the degree of

MASTER OF SCIENCE

Approved by:

Chair of Committee, Christine Ehlig-Economides
Committee Members, Ding Zhu
Karen Butler-Purry
Head of Department, Stephen Holditch

August 2007

Major Subject: Petroleum Engineering

ABSTRACT

Pressure Transient Test Analysis of Vuggy Naturally
Fractured Carbonate Reservoir: Field Case Study. (August 2007)
Babatunde Tolulope Ajayi, B.S., Bosphorus University
Chair of Advisory Committee: Dr. Christine Ehlig-Economides

Well pressure transient analysis is widely used in reservoir management to obtain reservoir information needed for reservoir simulation, damage identification, well optimization and stimulation evaluation. The main objective of this project is to analyze, interpret and categorize the pressure transient responses obtained from 22 wells in a vuggy naturally fractured carbonate reservoir in an attempt to understand the heterogeneities of the porosity system. Different modeling techniques useful in simulating well behavior in vuggy naturally fractured reservoirs were developed and categorized. The research focused on pressure transient analysis using homogeneous, radial composite, single fracture, dual porosity and triple porosity reservoir models along with conventional boundary models which show boundary limits including single and double sealing boundary, closure and constant pressure boundary. A triple porosity model was developed, and it proved to be very effective for use in the analysis of the pressure responses obtained from this field. For some wells, the need for new models to characterize the pressure responses in more complex reservoirs was highlighted as conventional models failed.

`

DEDICATION

I dedicate my thesis:

First to God for always being there for me and blessing me with strength and peace for every good work.

To my parents for their support and encouragement through the years

and

To my brothers for being good examples for me to emulate and for sharing their mistakes with me so that I wouldn’t make the same mistakes.

`

ACKNOWLEDGEMENTS

I would like to express my sincere gratitude and appreciation to my advising professor and committee chair, Dr Christine Ehlig-Economides for her support, guidance and help in completing this thesis. I would also like to acknowledge and thank Dr Ding Zhu and Dr Karen Butler-Purry for their support and service as members of my advisory committee. I would like to thank Dr Wayne Ahr for his guidance and intellectual contributions necessary for the completion of this thesis.

I would also like to thank the faculty and staff at the Harold Vance Department of Petroleum Engineering for their support and academic tutelage during my studies at Texas A&M University.

`

TABLE OF CONTENTS

Page

ABSTRACT iii

DEDICATION iv

ACKNOWLEDGEMENTS v

TABLE OF CONTENTS vi

LIST OF FIGURES viii

LIST OF TABLES xi

CHAPTER

I INTRODUCTION 1

1.1 Objectives 3
1.2 Problem Description 4
1.3 Scope of the Work 5

II PERSPECTIVES ON POROSITY IN CARBONATE RESERVOIRS 6

2.1 Complexity of Carbonate Pore System 6

III VUGGY NATURALLY FRACTURED RESERVOIRS 9

3.1 Fracture Properties 10
3.2 Classification of Fractured Reservoirs 14
3.3 Vugs 16
3.4 Caverns 18

IV WELL TEST ANALYSIS IN NATURALLY FRACTURED RESERVOIRS 19

V HOMOGENEOUS RESERVOIR MODEL 25

5.1 Introduction 25
5.2 Outer Boundary Conditions 34
5.3 Field Case Study 36

`

CHAPTER Page

VI SINGLE FRACTURE MODEL 41

6.1 Introduction 41
6.2 Wells Producing Next to a Single Major Fracture……………………..43
6.3 Wells Intersecting a Major Natural Fracture..46
6.4 Field Case Study..46

VII COMPOSITE RESERVOIR MODEL 49

7.1 Introduction 49
7.2 Field Case Study..51

VIII DUAL POROSITY MODEL 54

8.1 Double-Porosity Model with Pseudosteady-State Interporosity Flow...57
8.2 Field Case Study..60

IX TRIPLE POROSITY MODEL 63

9.1 Mathematical Model 64
9.2 Field Case Study..69

X FUTURE MODELS...75

XI CONCLUSIONS...79

NOMENCLATURE 83

REFERENCES 86

VITA 90

`

LIST OF FIGURES

FIGURE Page

2.1 Classification of Porosity (After Choquette And Pray[2]) 8

3.1 Schematic Plot of Fracture Porosity and Permeability Percentage for the Four Fractured Reservoir Types. (After Nelson[8]). 14

4.1 Ideal Model for a Naturally-Fractured Reservoir (after Warren and Root[3]). 20

4.2 Idealization of a Naturally-Fractured Reservoir (after Kazemi[14]).............. 21

4.3 Derivative Type Curve for Double-Porosity Reservoir, Pseudo-Steady State Flow (after Bourdet *et al*[22]). 23

4.4 Idealized Pressure Response in Quadruple Porosity Reservoirs (from Dreier *et al.*[26]). 24

5.1 Well Schematic Showing Fluid Flow into a Wellbore Located in the Center of a Homogeneous Reservoir................................ 26

5.2 Schematic of Radial Flow in a Homogeneous Cylindrical Reservoir......... 26

5.3 Schematic of Homogeneous Reservoir Types in NFR (after Cinco-Ley[12]) 27

5.4 Derivative Type Curve for Double Porosity Reservoir, Pseudo-Steady State Flow (after Bourdet *et al.*[19]). 30

5.5 Log-Log Plot of Designed Well Test 32

5.6 Semi-Log Plot of Designed Well Test 33

5.7 Log-Log Plot of Pressure Data from Well TW002 37

5.8 Semilog Graph of Pressure Data from Well TW002 38

6.1 Well Producing Next to a Single Fracture (a) and Well Intersecting a Single Fracture (b) 41

FIGURE Page

6.2 Flow Patterns Associated with Single Fracture Model (after Ehlig-Economides[22]) 42

6.3 Numerical Model of Well Next to Single Major Fracture 44

6.4 Semi-Log Graph of Well Next to Single Major Fracture............................44

6.5 Well Penetrating a Major Fracture Sensitivity to Fracture Half-Length......46

6.6 Log-Log Pressure and Derivative Curve for Well TW103 47

7.1 Radial Composite Naturally-Fractured Reservoirs 49

7.2 Derivative Type Curve of a Radial Composite Model With Varying M 50

7.3 Log-Log Pressure and Pressure Derivative Curve for Well TW009 51

7.4 Semilog Curve for Well TW009 52

8.1 Schematics for Dual Porosity Models..54

8.2 Typical Behavior of Dual Porosity Reservoir with Varying Omega Values..58

8.3 Typical Behavior of Dual Porosity Reservoir on Semi-Log Plot................59

8.4 Log-Log Pressure and Pressure Derivative Curve for Well TW004 61

8.5 Semi-Log Curve for Well TW004 61

9.1 Typical Behavior of Triple Porosity Reservoir with Varying Delta Values...67

9.2 Typical Behavior of Triple Porosity Reservoir on Semi-Log Curve 67

9.3 Triple Porosity Reservoir with Sensitivity to Matrix lambda Values……..68

9.4 Triple Porosity Reservoir with Sensitivity to Wellbore Storage…………..68

9.5 Log-Log Pressure and Pressure Derivative Curve for Well TW303 71

`

FIGURE Page

9.6 Semi-Log Curve for Well TW303 71

9.7 Dual-Porosity with Closure Boundary Match for Well TW303 73

9.8 Radial Composite Match for Well TW303 74

10.1 Pressure and Derivative Curve of Well TW017.. 75

10.2 Pressure and Derivative Curve of Well TW022.. 77

11.1 Distribution of Reservoir Models for Wells in Heterogeneous Vuggy NFR Field.. 81

LIST OF TABLES

TABLE Page

3.1 Characteristics and Examples of Type I to IV Fractured Reservoirs (adapted from Nelson[3]) 15

5.1 Pressure Transient Test Results for Well TW002 39

6.1 Numerical Modeling Results for Well Near a Major Fracture 46

6.2 Results of the Analysis of Well TW103 48

6.3 Results of the Analysis of Well TW009 53

8.1 Pressure Transient Analysis Solution of Well TW004 62

9.1 Results of the Analysis of Well TW303 72

10.1 Results of the Analysis of Well TW017 76

10.2 Results of the Analysis of Well TW022 78

11.1 Summary of Reservoir Models and Description Parameters 80

CHAPTER I

INTRODUCTION

A large fraction of the world’s natural hydrocarbon reserves can be found in carbonate reservoirs. Most of the world’s large oil reserves are in naturally fractured and vuggy carbonate reserves that have a complex, heterogeneous porosity system. About 22% of the oil reserves in the United States can be found in shallow-shelf carbonate reservoirs. Some of these include the Sprayberry field in West Texas and the Cottonwood creek field in Wyoming. The Yates field, located 90 miles south of Midland Texas is an example of a vuggy naturally fractured reservoir where the secondary-porosity flow features such as caves, solution-enhanced fractures and connected vugs have a large impact on the production and field development[1].

Carbonate reservoirs are especially susceptible to post-depositional diagenesis including dissolution, dolomitization and fracturing processes. These processes may enhance or negate fluid flow and reservoir quality. Processes such as dissolution have a positive effect on reservoir quality while cementation has a negative effect on reservoir quality. Most carbonate rocks have very little porosity but the few carbonate reservoirs that contain more than a few percent porosity are collectively of immense economic significance.

This thesis follows the style of the *SPE Reservoir Evaluation and Engineering Journal.*

`

Fracturing occurs when the rock fails because the differential forces acting upon it exceeds its elastic limit thereby causing a rupture. Fractures improve reservoir flow and connectivity.

Permeability within fractures is usually much higher than the permeability within the matrix and primary flow within the reservoir may be through the fracture system. Vugs, caverns and channels are created as a result of carbonate or sulfate dissolution. Vugs, caverns and channels also have an effect on the reservoir flow, connectivity and storativity. Vugs may result in high secondary porosity and may also contribute to primary flow if the vugs are interconnected.

Pressure transient tests can be used to interpret the characteristics of flow within a reservoir. These tests are based on the solution of the diffusivity equation satisfying appropriate boundary conditions. The time domain of interest is from a few seconds to a maximum of a few days. A number of authors have proposed different models for interpreting the pressure response from a naturally fractured reservoir but the complexity of porosity systems in a vuggy, naturally fractured reservoir require a model that accounts for the interaction between matrix, vug and fracture systems. New insights will be provided in this paper.

Production data analysis can be used to characterize the reservoir and interpret the cumulative production behavior in order to model the performance of the reservoir. The time domain of interest for reservoir performance modeling is from a few days to a few months to several years unlike the pressure transient tests. The presence of vugs and caves will also have a noticeable effect on the cumulative production behavior and it is necessary to incorporate vuggy porosity in the type-curve matching.

1.1 Objectives

The main objective of this project is to analyze, interpret and categorize the pressure transient responses observed in a vuggy naturally fractured carbonate reservoir in an attempt to understand the heterogeneities of the porosity system. The specific objectives are

1) To analyze and interpret well test data obtained from wells in a vuggy naturally fractured carbonate reservoirs using well test software,

2) To catalog modeling techniques useful in simulating well behavior in vuggy naturally fractured reservoirs

3) To ascertain the inadequacy of using conventional models found in commercial well test software to analyze more complex pressure responses obtained from some wells in the field,

4) To illustrate the use of triple porosity models to analyze well test data and

5) To combine production data analysis with pressure transient analysis as well as data obtained from drilling reports, geologic data, well logs and core samples to obtain unique interpretations for pressure responses obtained in a vuggy naturally fractured reservoir.

1.2 Problem Description

Well pressure transient analysis is a widely used in reservoir management to obtain reservoir information needed for damage identification, well optimization and stimulation evaluation. Well test analysis helps to understand the type of fluid flow within a reservoir as well as providing information necessary for other reservoir management processes such as numerical simulation. Some of the information obtained from pressure transient analysis include effective permeability, average reservoir pressure, distance to drainage area boundaries and skin.

The study starts with a comprehensive literature review to determine the current status of the knowledge of the porosity in vuggy naturally fractured reservoirs as well as the advancement of well test analysis in this kind of reservoir.

Well test data obtained from multiple wells in a vuggy naturally fractured field is analyzed using commercial well testing software. The different well test profiles are then analyzed using the pressure transient analysis models such as homogeneous, dual porosity and triple porosity models. Well test interpretations from the test field are then categorized according to reservoir and boundary model interpretations.

Pressure transient interpretations can be non-unique due to the complex porosity system found in vuggy naturally fractured reservoirs. It is therefore possible to obtain a good match for the pressure responses with various reservoir models. The multiple

`

interpretations of the well test data are made unique by comparing with additional information obtained from the geological map, production data, drilling logs and well logs.

1.3 Scope of the Work

The research is focused on pressure transient analysis using homogeneous, dual porosity and triple porosity reservoir models along with conventional boundary models which show boundary limits including single and double sealing boundary, closure and constant pressure boundary. Production data analysis is limited to obtaining reserve estimations and validating pressure transient interpretations. The characterization of fluid flow within large fluid filled caverns is not considered.

CHAPTER II

PERSPECTIVES ON POROSITY IN CARBONATE RESERVOIRS

Carbonate reservoirs generally have pore systems with complex geometry and genesis. It is important to be aware of the many possible stages in porosity evolution in order to analyze the formation. The genesis of porosity is well understood but there is limited knowledge of the many possible modifications to the porosity of a carbonate formation. Much of the porosity in carbonate reservoirs is created after deposition. Most of this porosity is created by processes of dissolution and dolomitization. A small fraction of the carbonate porosity that may dominate the flow behavior can be due to natural fractures.

2.1 Complexity of Carbonate Pore System

Pore spaces within carbonate formations tend to be complex both physically and genetically. Some sedimentary carbonates have porosity formed almost entirely from interparticle openings between nonporous grains of relatively uniform size and shape. This kind of porosity is relatively simple in geometry. This represents a simplicity that is uncommon in most sedimentary carbonates. In most carbonate formations, the size, shape, geometry of the pore openings as well as the nature of the boundaries show a lot of unpredictability.

The shape and size complexity of carbonates is caused by many factors. Some of the factors include a wide variation in the size and shape of the pores created by skeletal

`

secretion. This complexity is then increased greatly by solution processes and natural fracturing. Pore sizes range from 1micron or less in diameter to openings hundreds of feet across like the “Big Room” at the Carlsbad Caverns, New Mexico. The pore system created by dissolution could mimic porosity found in depositional particles or could be independent of both depositional particles and diagenetic crystal structure. Fracture openings can also strongly influence solution and are common in many carbonate formations.

Several time spans of porosity and several types of processes are responsible for the genesis of pores in the same formation. Biogenic processes include secretion of skeletal carbonate creating openings, spaces, chambers and cells. Mechanical porosity alterations include sediment packing, sediment shrinkage, sediment distention by gas evolution and rock fracturing. Further porosity alterations can be due to selective dissolution of sedimentary particles or the indiscriminate dissolution of the matrix, organic burrowing or boring, organic decomposition and many other ways. The formation of a pore could be a combination of any of these processes at different times. For example, consider a pore occupying the site of a shell that was dissolved selectively to form a mold, which then was filled completely with sparry calcite cement that resisted subsequent dolomitization of the matrix rock but later was dissolved selectively to form a second-generation mold. The final pore still reflects a positional and configuration controlled by the original shell.

`

According to Choquette and Pray[2], 15 basic porosity types are recognized: seven abundant types (interparticle, intraparticle, intercrystal, moldic, fenestral, fracture and vug) and eight more specialized types. Each type is classified by distinctive attributes such as pore size, pore shape, genesis, and position or association relative to overall fabric. The porosity types are classified on the basis of fabric-selective or non-fabric selective types. The non-fabric selective types are vugs, channels, fractures and caverns. Figure 2.1 shows the classification by Choquette and Pray[2].

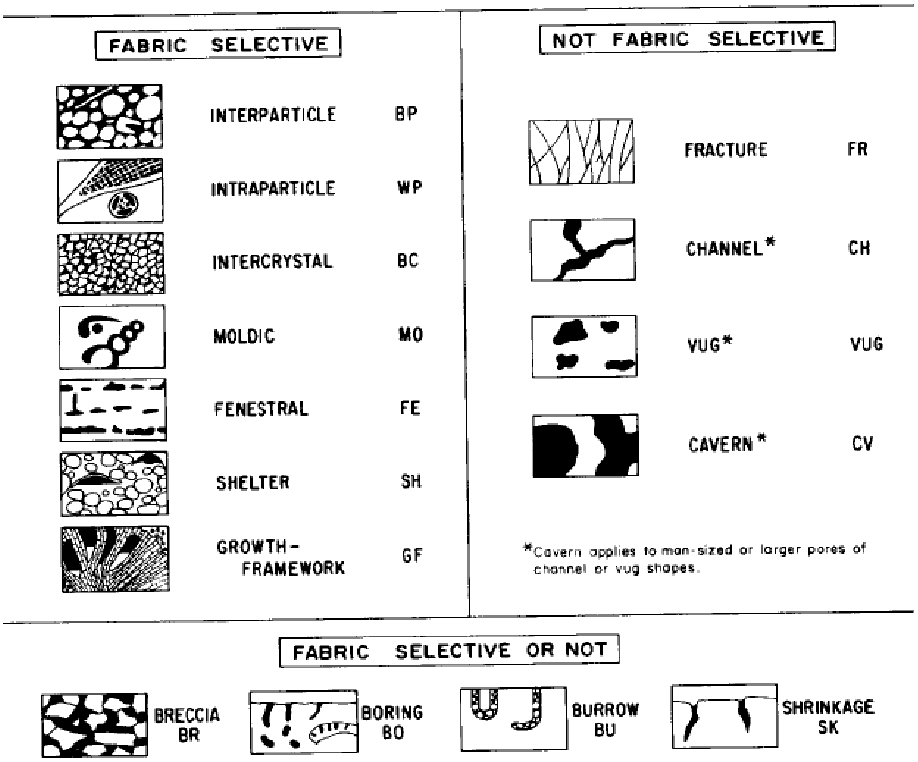
FABRIC SELECTIVE
INTERPARTICLE BP
INTRAPARTICLE WP
INTERCRYSTAL BC
MOLDIC MO
FENESTRAL FE
SHELTER SH
GROWTH-FRAMEWORK GF
NOT FABRIC SELECTIVE
FRACTURE FR
CHANNEL* CH
VUG* VUG
CAVERN* CV
*Cavern applies to man-sized or larger pores of channel or vug shapes.
FABRIC SELECTIVE OR NOT
BRECCIA BR
BORING BO
BURROW BU
SHRINKAGE SK

Figure 2.1: Classification of Porosity (after Choquette and Pray[2])

CHAPTER III

VUGGY NATURALLY FRACTURED RESERVOIRS

Vuggy naturally fractured reservoirs are reservoirs in which natural fractures as well as large or small vugs have, or are predicted to have, a significant effect on fluid flow in terms of increased reservoir permeability, reserves or increased permeability anisotropy.

Vuggy fractures are enlargements within and along natural fractures where undersaturated fluids have removed the rock matrix. Enlargement of vuggy fracture systems occurs commonly due to water percolating from unconformities and some vuggy fractures are related to karst systems.

Nelson, R. A[3] defined fractures as naturally occurring macroscopic planar discontinuities in rock due to geomechanical deformation or physical diagenesis. Geomechanical fractures are created either by brittle or ductile failures. Brittle failures occur when the rocks fail by rupture under differential stresses. Rocks behave as brittle materials at low temperatures and confining pressures such as the earth's surface or relatively shallow burial depths.

Fracture characteristics differ depending on the genesis of the fracture. In highly deformed rocks, multiple generations of fracturing may occur in which older fractures may be overprinted by younger ones. Fractures can have positive or negative effects on fluid flow and reservoir performance. Some fractures may be partially or completely

`

filled by diagenetic precipitates after fracturing effectively decreasing the porosity. Nelson[8] has stressed the importance of collecting information that allows the identification of a reservoir as fractured in early stages of development in order to properly manage and take advantage of the fractures in the reservoir.

The field case examples were obtained from an Ordovician carbonate reservoir with almost zero matrix permeability. The matrix porosity obtained from core samples was determined to be less than 3%. Flow in the reservoir seems to occur mainly through natural fractures, and producible fluids may be stored mainly in vugs.

3.1 Fracture Properties

For effective characterization of naturally fractured reservoirs, two major factors have been identified to govern permeability and porosity of fractures. These reservoir parameters are fracture width and spacing. Fracture width (e) is the distance between two parallel surfaces that represent the fracture. Fracture spacing (D) is the average distance between parallel regularly spaced fractures.

According to Nelson[3], the four most relevant properties of fractured reservoirs, in order of increasing difficulty to determine, are fracture porosity, fracture permeability, fluid saturation within fractures, and the recovery factor expected from the fracture system. Calculations obtained from wireline log data do not provide accurate information for the evaluation of fracture contributions to reservoir performance. Image logs such as

Schlumberger FMI® (Formation Microresistivity Imaging log) and FMS® (Formation Microscanning log) are useful for fracture identification and also for determining the orientation, thickness, and spacing of the fractures. However, image logs cannot indicate whether fractures are open or cemented, and it is useful to accompany the image logs with acoustic logs to this distinction.

Fracture Porosity

Fracture porosity is a percentage of void space in fractures compared to the total volume of the system. Fracture porosity is estimated using the following equation:

$$\phi_f = \frac{e}{D+e} \times 100\% \quad \text{..3.1}$$

ϕ_f = Fracture porosity

e = average effective fracture width

D = average spacing between parallel fractures

It should be noticed that fracture porosity is scale dependent since a constant fracture width, e, varies as a function of distance between fractures. This means that fracture porosity can be a 100% in a specific location in the reservoir while the average porosity for the reservoir as a whole can be as low as 1%. According to Nelson[3], fracture porosity is always less than 2%; in most reservoirs it is less than 1%. Vuggy fractures however

`

are an exception to this rule because porosity in vuggy fractures can vary from 0 to very large percentages.

In vuggy natural fractured reservoirs, the fracture system provides relatively little porosity but essential permeability to the reservoir; whereas the system of vugs can provide essential porosity for the reservoir. This makes the fracture and vug porosity a critical factor to be considered in early stages of reservoir development.

Matrix porosity is expressed as a percentage of the matrix pore volume to the total volume of the rock.

$$\phi_m = \left(\frac{V_p}{V_t}\right) \times 100\% \ldots\ldots\ldots\ldots\ldots\ldots\ldots\ldots\ldots\ldots\ldots 3.2$$

Where V_p is the volume of the pores in the matrix while V_t is the total sample volume which is the sum of the pore volume and the total solid rock volume.

As contribution of matrix porosity to the whole system increases, the relevance to storage capacity of fracture porosity decreases. Similarly, as the contribution of vuggy porosity increases, the relevance of the fracture porosity decreases. The estimation of fracture porosity in early stages is not so vital in reservoirs where matrix porosity is several orders of magnitude greater than fracture porosity. Some vuggy naturally fractures reservoirs have been known to have large vugs and cavern porosity such that

`

the secondary porosity within the vugs may be several orders of magnitude greater than matrix porosity.

Fracture Permeability

Permeability is a parameter for evaluating the ability if a porous medium to allow the flow of fluid through it. Very high permeability through connected vugs, fissures and fractures is relatively common in many carbonate rocks.

Many models have failed to describe fluid flow in fractures because they have been based on Darcy's equation. Darcy's equation can not be used to accurately define flow through fractures. In order to model fluid flow in fractures, Warren and Root[4] developed the double-porosity model.

`

3.2 Classification of Fractured Reservoirs

Nelson[3] proposed the classification of fractured reservoirs into four types according to their effect the fractures have on reservoir performance:

Type 1: Fractures provide the essential reservoir porosity and permeability.

Type 2: Fractures provide the essential reservoir permeability.

Type 3: Fractures assist permeability in an already producible reservoir.

Type 4: Fractures provide no additional porosity or permeability but create significant reservoir anisotropy, such as barriers to flow.

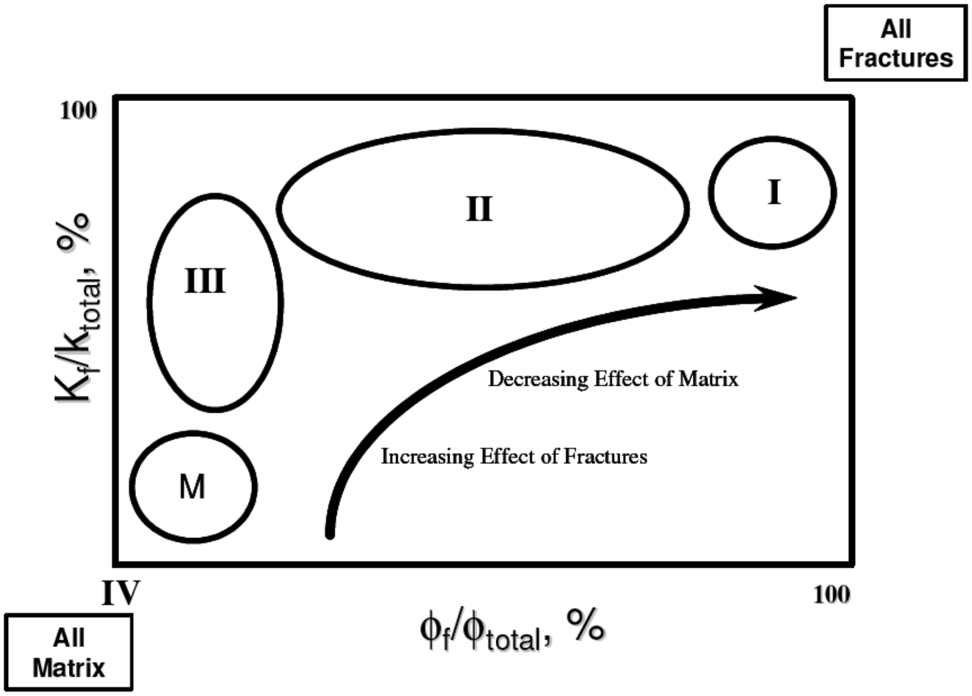
All Fractures
100
K_f/k_{total}, %
II
I
III
Decreasing Effect of Matrix
Increasing Effect of Fractures
M
IV
100
ϕ_f/ϕ_{total}, %
All Matrix

Figure 3.1: Schematic Plot of Fracture Porosity and Permeability Percentage for the Four Fractured Reservoir Types. (After Nelson[3]).

`

It can be seen from Figure 3.1 that the effect of fractures is of paramount importance for Type 1 reservoirs, decreases for Type 2 and so on. In the same way, the importance of proper characterization of porosity and permeability changes with reservoir type. Type M in Figure 3.1 is representative of conventional matrix reservoirs and Type IV reservoirs show the same characteristics as the conventional matrix reservoirs with fractures acting as heterogeneities. The vuggy naturally fractured reservoir that is examined in this project is considered to be a Type 1 reservoir because there is ample evidence to suggest a strong influence of vugs and fractures on the porosity and permeability of the reservoir. Table 3.1 gives the characteristics and examples of the different reservoir types.

Table 3.1: Characteristics and Examples of Type I to IV Fractured Reservoirs (adapted from Nelson[8])

Reservoir Type	**Characteristics**	**Problems**	**Field Examples**
Type 1 Fractures provide essential porosity-permeability	Large drainage areas per well Few wells needed for development Good reservoir quality-well information correlation Easy good well location Identification High initial potential	Rapid decline rates Possible early water encroachment Size/shape drainage area difficult to determine Reserves estimation complex Additional wells accelerate but not add reserves	Amal, Libia Ellenburger, Texas Edison, California Wolf Springs, Montana Big Sandy, Kentucky
Type 2 Fractures provide essential permeability	Can develop low permeability rocks Well rates higher than anticipated Hydrocarbon charge often facilitated by fractures	Poor matrix recovery (poor fracture-matrix communication) Poor performance on secondary recovery Possible early water encroachment Recovery factor variable and difficult to determine	Agha Jari, Iran Hart Kel, Iran Rangely, Colorado Spraberry, Texas La Paz/Mara, Venezuela

`

Table 3.2: Continued

Reservoir Type	Characteristics	Problems	Field Examples
Type 3 Fractures provide permeability assist	Reserves dominated by matrix properties Reserve distribution fairly homogeneous High sustained well rates Great reservoir continuity	Highly anisotropic permeability Unusual response in secondary recovery Drainage areas often highly elliptical Interconnected reservoirs Poor log/core analysis correlation Poor well test performance	Kirkuk, Iraq Gachsaran, Iran Hassi Mesaoud, Algeria Dukhan, Qatar Lacq, France Cottonwood Creek, Wyoming
Type 4 Fractures create flow barriers	Reservoir typically compartmentalized Permeability anisotropy may be unlike that in adjacent fractured reservoirs with different fracture style	Wells underperform compared to matrix capabilities Recovery factor highly variable across field	

3.3 Vugs

Choquette and Pray[1] described vugs as equant pores which are large enough to be seen with the naked eye, but do not specifically conform in position, shape or boundary to grains within the host rock. Lucia[5] stated that vugs are pores that are significantly larger than framework grains.

Vugs are formed due to carbonate or sulfate dissolution. Vuggy porosity is common in many reservoirs, and it is an important factor to be considered when studying the petrophysical characteristics of a reservoir rock. The determination of permeability and porosity in vuggy zones is likely to be pessimistic because of sampling problems. It is very difficult to acquire enough samples to give an accurate estimation of permeability

`

and porosity for vuggy reservoirs. In areas where core samples are not available, open-hole wireline logs may be used to identify vuggy zones. However, vugs are not always recognized by conventional wireline logs because of their limited vertical resolution. Quintero *et al.*[6] explains that even though open fractures and well connected vugs have a dramatic influence on total permeability; nuclear magnetic resonance (NMR) tools will be responsive to matrix permeability while being insensitive to open fracture and well connected vugs. The effect of vugs on permeability is based on their connectivity. Vuggy permeability is very important in some reservoirs. In some reservoirs vuggy permeability may be even more important than fracture permeability and fractures may be considered secondary in their effect on permeability in vuggy zones.

Casar-Gonzalez and Suro-Perez[7] investigated porosity and permeability in vuggy zones using x-ray computed tomography. They found that the concentric halos surrounding vugs have enhanced matrix porosity and permeability. Porosity and permeability enhancement within the reservoir may be caused by vugs connected directly and by vugs connected through the zones of slightly enhanced matrix porosity and permeability surrounding them. These halos are concentric around the vugs and porosity decreases from vug centers to the extremes. The permeability around the concentric halos was measured to be as high as 700md whereas lower values were measured for the regions of the core farther away from the vugs[8]. This observation suggests that the halos improve interconnectivity of the vugs.

`

Neale and Nader[9] proposed a model to evaluate vuggy permeability. The model proposed involved defining the vuggy zone as two regions. The creeping Navier Stokes equation is used within a spherical cavity and the Darcy equation is used to calculate the flow in the surrounding porous medium. The resulting equation produces a relation between the matrix and the system permeability of the vuggy porous medium is given in reference 9.

3.4 Caverns

Although most caverns in carbonate rocks is of solution origin, the porosity is classified as cavern porosity based on the size of the opening only and not on the origin. The size of the opening has to be large enough to warrant designation as a cavern. A practical lower size limit of cavern porosity for outcrop studies is about the smallest opening an adult person can enter[2].

A practical lower size limit from a drilling standpoint is the an opening large enough to cause easily recognizable drop of the drilling bit (a half meter or so). Subsurface cores of the usual diameter of only 7-12cm cannot be used to identify cavern porosity. Cavern openings can be as large as hundreds of meters across like the “Big Room” at Carlsbad Caverns, New Mexico.

CHAPTER IV

WELL TEST ANALYSIS IN NATURALLY FRACTURED RESERVOIRS

Numerous models have been proposed to represent naturally fractured reservoirs; however the dual porosity model is the most widely accepted in the petroleum industry.

Cinco-Ley[10,11] described well testing as an ideal tool to find reservoir-flow parameters and to detect and evaluate heterogeneities that affect the flow process in carbonate formations. He discussed five different reservoir flow models that can be used to portray the behavior of naturally fractured reservoirs. The models are homogeneous reservoir, composite reservoir, anisotropic medium, single fracture system and double porosity medium. The paper discussed the application and limitations of these models in well-test analysis.

Warren and Root[4] introduced the concept of dual porosity behavior to petroleum industry. They developed an idealized analytical solution for single-phase, compressible fluid flow in heterogeneous reservoirs. The model consists of representing the reservoir as being composed of rectangular parallelepipeds where the blocks represent the matrix and the space in between represents the fractures as illustrated in Figure 4.1. The fractures are assumed to have low storage and high permeability while the matrix is assumed to have high storage and low permeability. Fluid flow was assumed to occur only through the fracture system while the matrix acts only as a fluid source for the fracture system. The flow from matrix to fractures is assumed to be pseudosteady state.

`

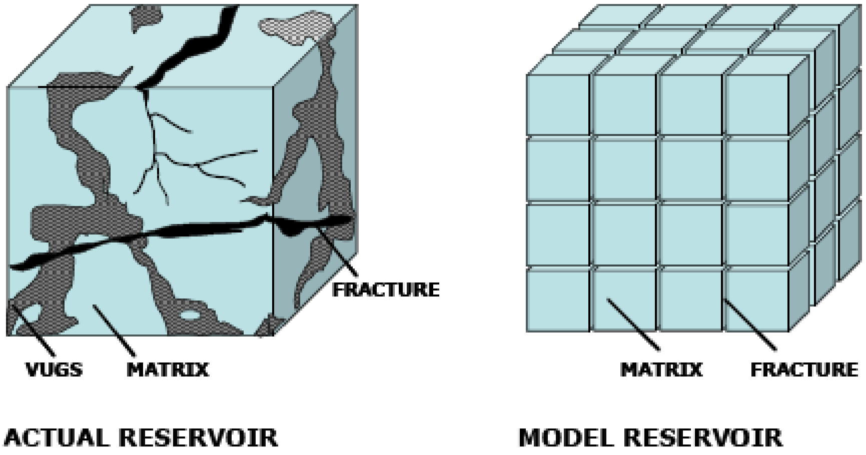

Figure 4.1: Ideal Model for a Naturally Fractured Reservoir (after Warren and Root[4]).

Warren and Root[4] assumed that naturally fractured reservoirs can be characterized by the same parameters for homogeneous reservoirs with two additional parameters and they show that the pressure transient response for this type of reservoir could be represented by two parallel semilog straight lines.

Kazemi[12] presented a model similar to the Warren and Root model for naturally fractured reservoirs based on transient interporosity flow in the matrix. He used numerical solutions of an idealized circular finite reservoir with a centrally located well where all the fractures are assumed to be horizontal. Figure 4.2 shows the Kazemi idealized model. The model assumes unsteady state single phase flow in radial and vertical directions from the matrix (high storage capacity and low flow capacity) to the fracture (low storage capacity and high flow capacity).

`

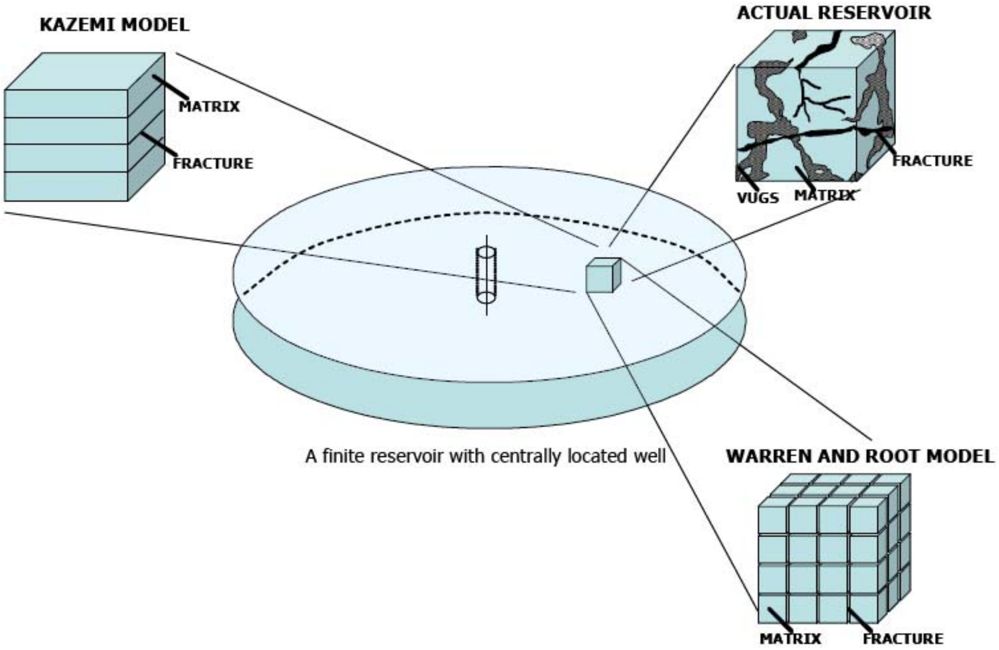
KAZEMI MODEL
MATRIX
FRACTURE
ACTUAL RESERVOIR
FRACTURE
VUGS
MATRIX
A finite reservoir with centrally located well
WARREN AND ROOT MODEL
MATRIX
FRACTURE

Figure 4.2: Idealization of a Naturally Fractured Reservoir (after Kazemi[12]).

The solutions obtained showed three parallel semilog straight lines, the first and third semilog lines are equivalent to that of Warren and Root[4]. His solutions are similar to those of Warren and Root[4], the only major difference is the transition period between fracture flow and the total system flow corresponding to the second semilog line. Kazemi[11] concluded that the Warren and Root[4] model for naturally fractured reservoirs is valid for unsteady flow and that the value of the interporosity flow coefficient is dependent on the matrix-to-fracture flow regime.

De-Swaan[13] developed an analytical double-porosity model assuming transient interporosity flow in the matrix for different geometries than those used by Kazemi[14]. He

`

presented early and late time region solutions for spherical and slabs idealized models but the solutions for the transient period was not presented.

Najurieta[14] extended the solutions presented by De Swaan[13] in order to properly describe the transitional period taking into account the transient behavior in the matrix. He presented a simplified model for slabs and cubes idealized models and he also proposed a systematic approach for analyzing well tests in naturally fractured reservoirs.

Bourdet and Gringarten[15] proposed a new set of type curves for analyzing wells with wellbore storage and skin effects in dual porosity systems. They developed the type curves by rearranging the parameter combinations in the solutions presented by Mavor and Cinco-L.[11]. Gringarten[16] illustrated the application of these type curves to evaluate matrix block size and fissure volume in fissured reservoirs from actual well test data.

Bourdet *et al.*[17,18] introduced the use of pressure-derivative type curves in well-test in naturally fractured reservoirs interpretation and discussed the application of the new type curves to interpret well test data. An example of the derivative type curve is shown in Figure 4.3. They showed the use of the derivative pressure curve as diagnostic plots in performing well test analysis. For NFR, they considered both pseudosteady-state and transient flow and the effects of wellbore storage and skin was included. Several field examples were illustrated.

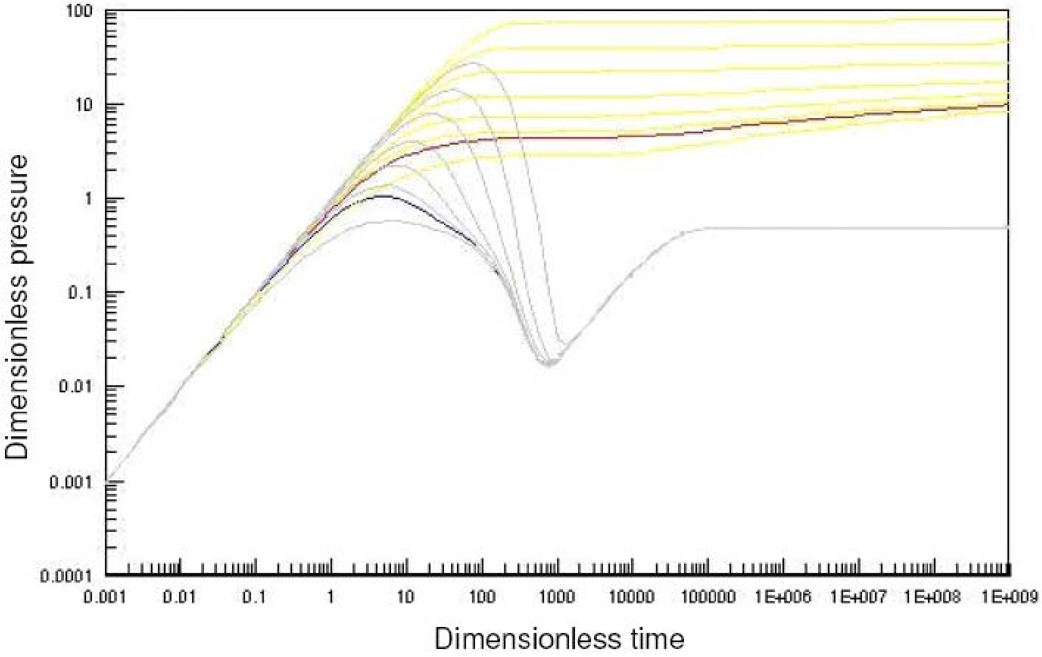

Figure 4.3: Derivative Type Curve for Double-Porosity Reservoir, Pseudo-Steady State Flow (after Bourdet *et al*[18]).

A number of authors have discussed the inability of the dual-porosity model to account for more complex reservoirs. Abdassah and Ershaghi[19] proposed the first triple-porosity/ single-permeability model in 1986. These authors considered an unsteady state interporosity flow model between the fracture system and two types of matrix blocks. Primary flow is assumed to occur only through the fracture system.

Camacho-Velazquez et al[7] proposed a triple-porosity/ dual- permeability model that accounts for primary fluid flow within the system of interconnected vugs to the well in

`

addition to the flow through the fractures since touching vugs contribute to both effective porosity and permeability. Dreier *et al.*[20] presented two quadruple porosity models in 2004. Figure 4.4 shows an example of the pressure and derivative curve response in a quadruple porosity system presented by Dreier *et al.*[20].

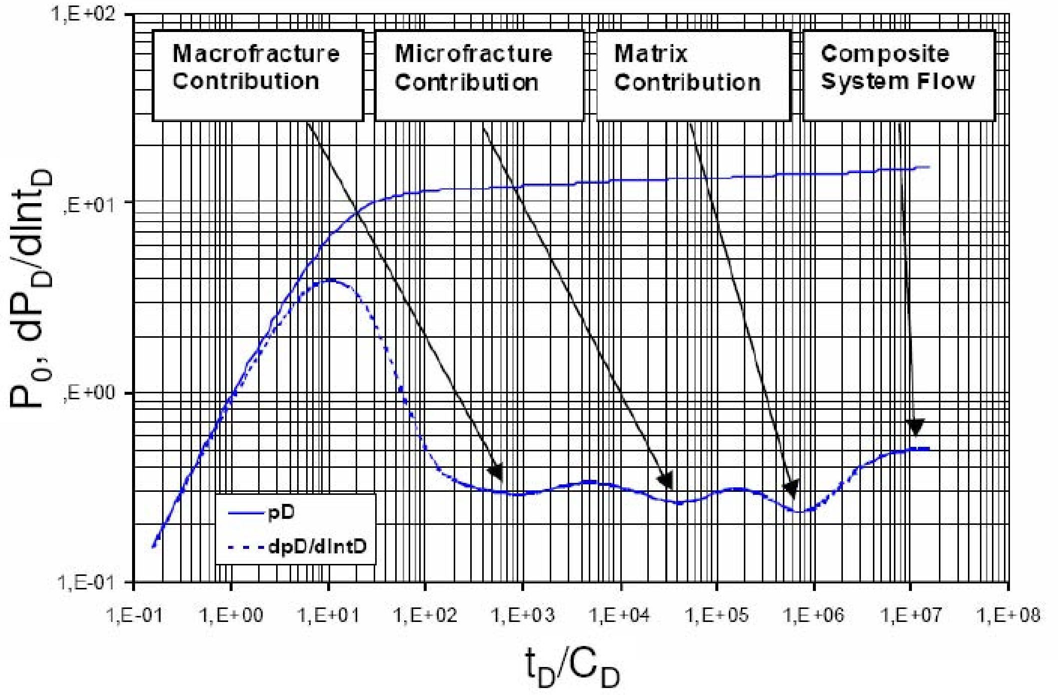

Figure 4.4: Idealized Pressure Response in Quadruple Porosity Reservoirs (from Dreier *et al.*[20]).

`

CHAPTER V

HOMOGENEOUS RESERVOIR MODEL

5.1 Introduction

In this chapter, the use of the homogeneous reservoir model to analyze the pressure response obtained from a build-up or drawdown test in a well drilled into a vuggy naturally fractured reservoir is considered. Figure 5.1 illustrates the fluid flow into a wellbore located in the center of a homogeneous reservoir.

The homogeneous reservoir model assumes that the reservoir properties are constant and do not vary throughout the reservoir[21]. The specific assumptions of the model are:

- slightly compressible fluid
- uniform pressure, p_i, in the drainage area of the well
- sufficient homogeneity so that the radial-diffusivity equation adequately models reservoir flow (Figure 5.2)
- production at a constant withdrawal rate, q ,
- the reservoir is infinitely acting until a boundary is encountered

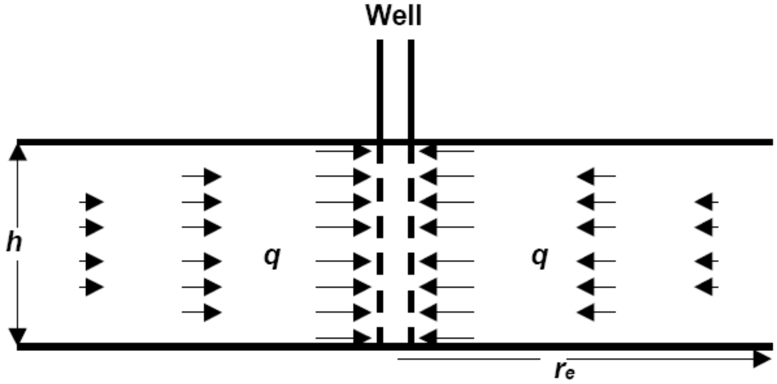

Figure 5.1: Well Schematic Showing Fluid Flow into a Wellbore Located in the Center of a Homogeneous Reservoir.

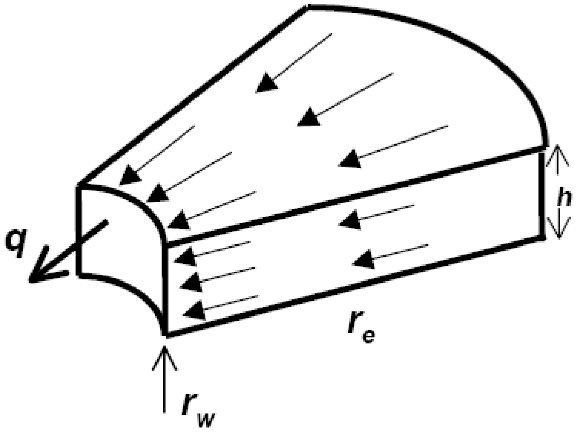

Figure 5.2: Schematic of Radial Flow in a Homogeneous Cylindrical Reservoir.

In vuggy naturally fractured reservoirs, the homogeneous reservoir model assumes that the fracture, matrix and vugular systems act as one continuous medium such that fluid flow between them occurs instantly without resistance. Reservoir fluid production occurs simultaneously from the multiple porosity system. The homogeneous behavior is normally exhibited by either a heavily fractured and vuggy reservoir with small matrix blocks as in diagram (a) in Figure 5.3 or by a vuggy naturally fractured reservoir where the fluid are contained mainly in the natural fractures or connected vugs shown in diagram (b) in Figure 5.3 .

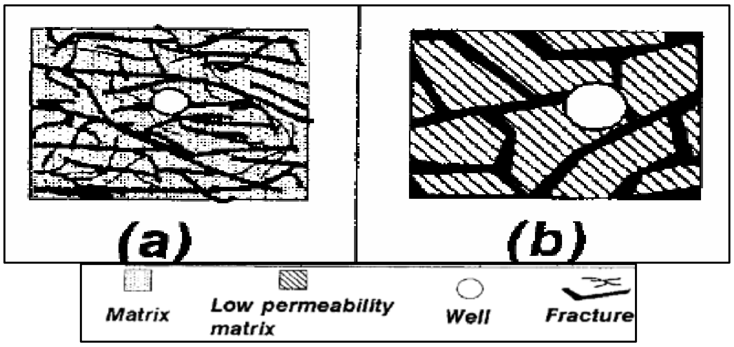

Figure 5.3: Schematic of Homogeneous Reservoir Types in NFR (after Cinco-Ley[10])

An illustration of these examples can be seen in Figure 5.3. Some wells have been known to be highly productive from a reservoir with low hydrocarbon reserves. In this case, the fluid is contained mainly in the fractures and the system therefore behaves as a homogeneous medium.

Conventional pressure transient test solutions focused on the homogeneous reservoir solution and several pressure transient analysis methods have been developed and discussed extensively in literature[21,22]. In general, pressure response behavior is controlled by the formation flow capacity kh, porosity ϕ, fluid viscosity μ and total compressibility, c_t.

`

In order to properly analyze pressure data, two complimentary approaches are used. The first approach involves the global flow-regime diagnosis achieved by the application of a log-log graph of both the pressure and the pressure derivative. This process helps to identify the characteristic flow regimes, allows the detection of flow geometries and the presence of heterogeneities in the system.

The second approach involves the specialized analysis of specific flow regimes. Selected portions of the pressure data are analyzed and reservoir flow parameters are obtained from the analysis. Both approaches have to be performed concurrently and the results must be consistent.

Diagnosis of pressure behavior can be performed by type curve analysis. Type curves are usually represented as dimensional variables instead of real variables for convenience sake.

Consider the line-source solution for slightly compressible fluids with added skin factor variable.

$$p_i - p_{wf} = -\frac{70.6qB\mu}{kh}\left[Ei\left(-\frac{948\phi\mu c_t r^2{}_w}{kt}\right) - 2s\right] \text{………………………..5 .1}$$

Dimensionless variables are defined as:

$$p_D = \frac{kh(p_i - p)}{141.2qB\mu} \text{……………………………………..5 .2}$$

`

$$r_D = \frac{r}{r_w} \quad \ldots\ldots\ldots\ldots\ldots\ldots\ldots\ldots\ldots\ldots\ldots\ldots 5.3$$

$$t_D = \frac{0.0002637kt}{\phi\mu c_t r^2{}_w} \quad \ldots\ldots\ldots\ldots\ldots\ldots\ldots\ldots\ldots\ldots\ldots 5.4$$

Substituting the dimensional variables into the line source yields

$$p_D = -\frac{1}{2}Ei\left(\frac{-r^2{}_D}{4t_D}\right) + s \quad \ldots\ldots\ldots\ldots\ldots\ldots\ldots\ldots\ldots 5.5$$

Bourdet et al[18] developed a type curve shown in Figure 5.4 which includes a pressure derivative function based on the analytical solution derived by Agarwal et al[23] and plotted on the type curves generated by Gringarten et al[24].

Dimensionless pressure, P_D is plotted on a log-log scale against dimensionless time group, t_D/C_D. Also the dimensionless $P'_D(t_D/C_D)$ is plotted as a function of t_D/C_D. The derivative is defined as:

$$P'_D = \frac{dP_D}{d(t_D/C_D)} \quad \ldots\ldots\ldots\ldots\ldots\ldots\ldots\ldots\ldots\ldots\ldots 5.6$$

`

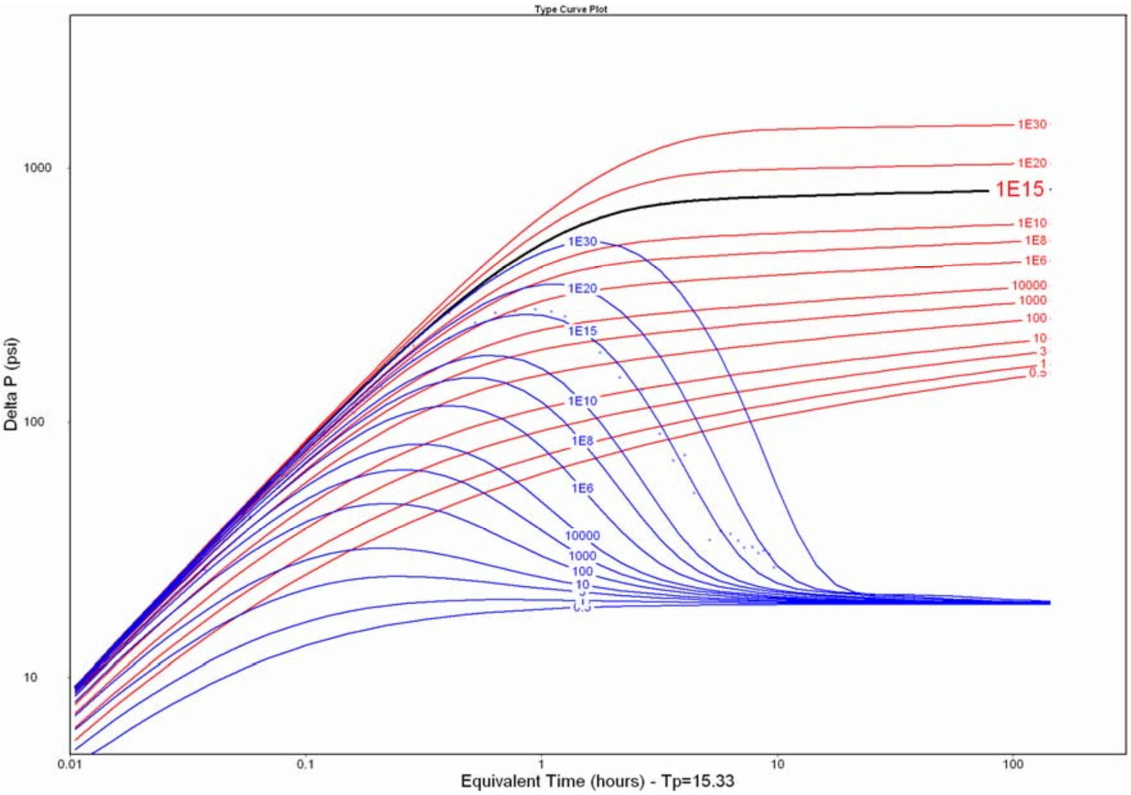

Figure 5.4: Derivative Type Curve for Double-Porosity Reservoir, Pseudo-Steady State Flow. (after Bourdet *et al*.[19]).

Two flow regimes of interest can be identified in the pressure response. At the early time region, for well test data on a unit slope-line corresponding to pure well-bore storage effect.

$$P_D = t_D / C_D \ldots\ldots\ldots\ldots\ldots\ldots\ldots\ldots 5.7$$

$$\frac{dp_D}{d(t_D / C_D)} = p'_D = 1 \ldots\ldots\ldots\ldots\ldots\ldots\ldots\ldots 5.8$$

$$p'_D (t_D / C_D) = t_D / C_D \ldots\ldots\ldots\ldots\ldots\ldots\ldots\ldots 5.9$$

Then,

$$\log p'_D (t_D / C_D) = \log t_D / C_D \ldots\ldots\ldots\ldots\ldots\ldots\ldots\ldots 5.10$$

`

The slope of the derivative curve on a log-log graph is unity. Consequently, at early times on a log-log graph, a type-curve plot of the pressure should coincide with the plot of the pressure derivative if the early data are distorted by wellbore storage and are characterized by a unit-slope line.

The test data can be plotted on the semi-log straight line. When all the wellbore storage is over, the constant sandface flow rate is established. Radial flow is characterized by a straight line on a semilog plot. Dimensionless pressure can be modeled with the logarithmic approximation to the line source solution.

$$Ei(-x) \approx \ln(1.781x) \tag{5 .11}$$

This approximation simplifies the line-source solution including the skin factor, to

$$p_D = 0.5(\ln t_D + 0.80907 + 2s) \tag{5 .12}$$

Adding and subtracting $\ln C_D$ into equation 5 .11 yields

$$p_D = 0.5[\ln(t_D - \ln C_D + 0.80907 + \ln(C_D e^{2s})] \tag{5 .13}$$

Then,

$$\frac{dp_D}{d(t_D / C_D)} = p'_D = \frac{0.5}{(t_D / C_D)} \tag{5 .14}$$

$$p'_D (t_D / C_D) = 0.5 \tag{5 .15}$$

This indicates the pressure derivative from the middle time region of a semilog straight line will follow a level trend on the derivative type curve. This flow region is known as the infinite acting radial flow regime. Figure 5.5 and Figure 5.6 illustrate the behavior of a single well test. The pressure response shows wellbore storage and skin in homogeneous reservoir model.

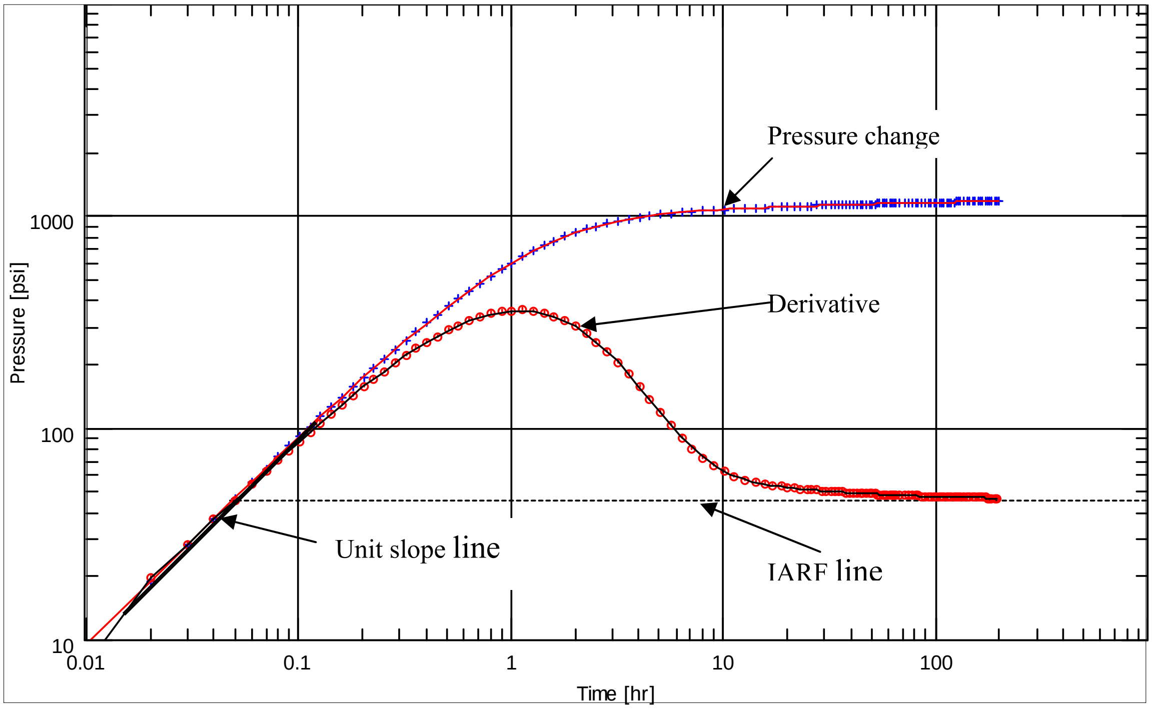

Figure 5.5: Log-Log Plot of Designed Well Test

`

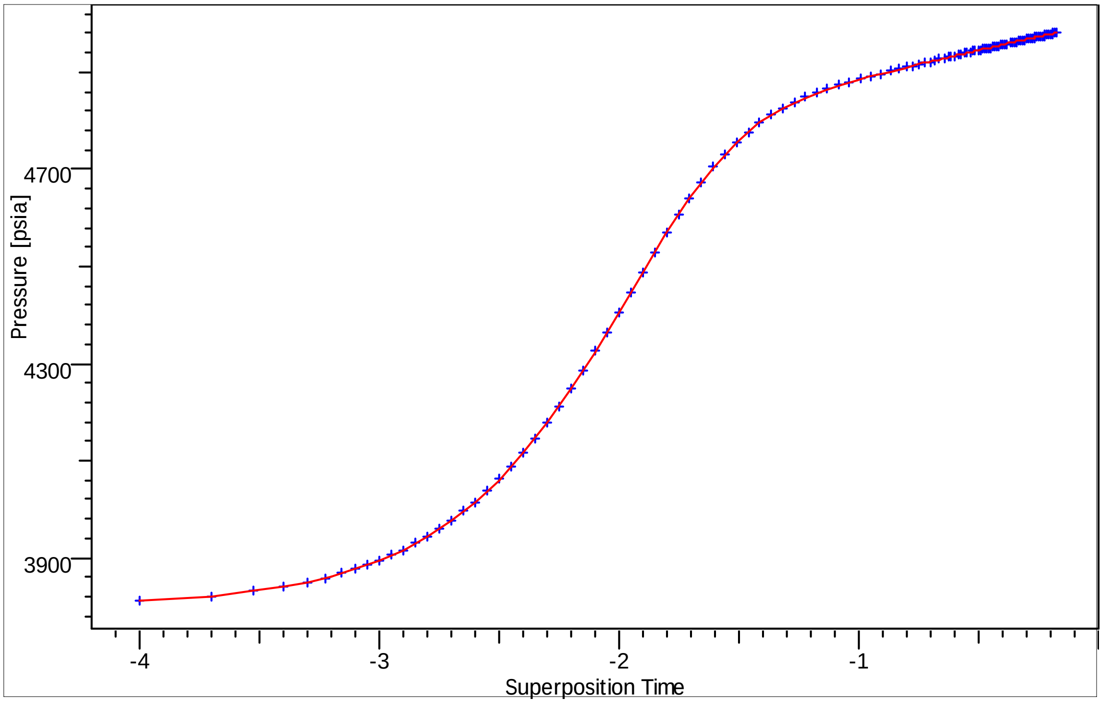

Figure 5.6: Semi-Log Plot of Designed Well Test

The permeability, k, can be calculated from the pressure match point on the derivative curve.

$$k = \frac{70.6qB\mu}{m'h} \quad \ldots\ldots 5.16$$

Where , m' is the level of the derivative at match point, that is

$$m' = \left(\frac{p_D}{\Delta p}\right)_{matchpoint} \quad \ldots\ldots 5.17$$

The skin factor, s, can be calculated below from the match point.

`

$$s = 1.151\left[\frac{\Delta p_{ws}}{2.303m'} - \log\frac{k}{\phi\mu c_t r_w^2} + 3.23 + \log\left(\frac{t_p + \Delta t}{t_p}\right) - \log\Delta t\right] \text{................}5\ .18$$

for $\Delta p_{ws}, \Delta\text{t}$ in IARF, where

$$\Delta p_{ws} = p_{ws} - p_{wf}(t_p) \text{.................................}5\ .19$$

$$p^* = m'\ln\left(\frac{t_p + \Delta t}{\Delta t}\right) + \Delta p_{ws} + p_{wf}(t_p) \text{.............................}5\ .20$$

for $\Delta p_{ws}, \Delta\text{t}$ in IARF

The dimensionless wellbore storage coefficient, C_D, can be calculated from the time match point and compared with the value computed from the unit slope line if a unit slope line is present.

$$C_D = \frac{0.0002637k}{\phi h c_t r^2{}_w}\left(\frac{t \text{ or } \Delta t_e}{t_D / C_D}\right)_{matchpo\,\text{int}} \text{..............................}5\ .21$$

5.2 Outer Boundary Conditions

Boundary effects are usually difficult to observe in pressure transient analysis curves because they occur at the late time period. During this period, the amplitude of the pressure change is large, whereas the changes of trend are slow. Boundary effects are generally only present in a small portion of the data curve on a logarithmic scale due to the compression that occurs on the logarithmic scale. In order to observe boundary effects in well tests, it may be necessary to shut down the well longer than desirable. Pressure derivative curves are useful in identifying boundary effects.

`

A single sealing fault near the producing well can be observed in late time data when the derivative curve stabilizes into a straight line first at 0.5 (radial flow) then doubles and settles later at 1. The slope of the semi-log straight line doubles. For parallel sealing faults, linear flow occurs and is observed as straight lines with a slope of ½ both on the pressure and derivative curves. The derivative response curve however tends to produce the ½ slope straight line earlier in time than the pressure response. Two sealing faults intersecting at an angle θ would cause the late time derivative curve to settle later at a level $2\pi/\theta$ after stabilizing first at straight line level 0.5 (infinitely acting radial flow). The transition between the two constant derivative levels is a function of the location of the well relative to the angle.

In the case of a well in a closed system, the pseudo-steady state flow occurs in late time and the pressure variation is proportionate to time. The closed system can be modeled analytically as a circular or rectangular no-flow closure boundary, however a closed system could be due to any shape of closure as long as the well is draining from a limited reservoir area. Interference from other wells producing from the same reservoir may appear in the pressure response as a no-flow boundary. In pressure drawdowns, the log-log plot of both the pressure and the pressure derivative against time tends to an asymptote with a slope of unity. The derivative curve tends to rise with a unity slope earlier in time than the pressure curve. However, in pressure buildups, the log-log plot of the derivative falls steeply. In diagnosing closed system, it is important to note that the rise in the pressure curve can take place over more than one log cycle on the time scale.

`

In the case of constant pressure boundaries, the pressure curve stabilizes while the pressure derivative drops sharply. In cases of heterogeneous reservoirs, boundary effects are known to produce complex pressure responses. The use of the pressure curve alone can make the interpretation very difficult. The derivative curve has proven to be very useful in the interpretation of the well behavior.

5.3 Field Case Study

An analysis of the pressure transient test data obtained from different wells in the study field indicates that 9 out of 22 wells tested showed homogeneous reservoir behavior with varying wellbore storage, skin effects and boundary conditions.

A 470 hour build-up was performed on test well TW002 serves as an example. Commercial well test software, Ecrin® was used for computation, regression and test analysis. Figure 5.7 and 5.8 shows the plot of the pressure and pressure derivative against time on a logarithmic scale. The pressure and input data was corrected for scatter and inconsistencies. This was done by synchronizing initial start time of the buildup pressure data by adjusting it to match the time at the start of the pressure buildup.

An examination of the derivative curve reveals three specific flow regimes: wellbore storage at the early time region characterized by a unit slope in both the pressure and the pressure derivative curve, infinite acting radial flow at the middle time region

`

characterized by a horizontal straight line in the derivative curve and the presence of 2 parallel no-flow boundaries in the late time region characterized by a derivative curve rising with a half slope.

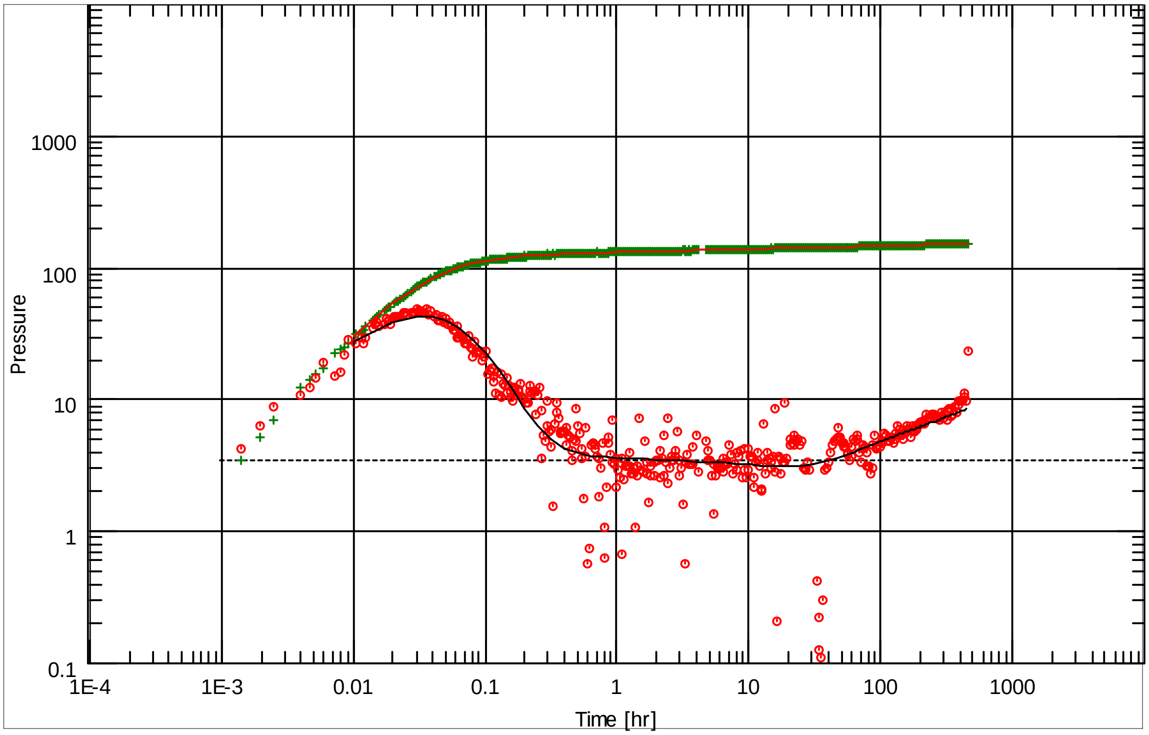

Figure 5.7: Log-Log Plot of Pressure Data from Well TW002

`

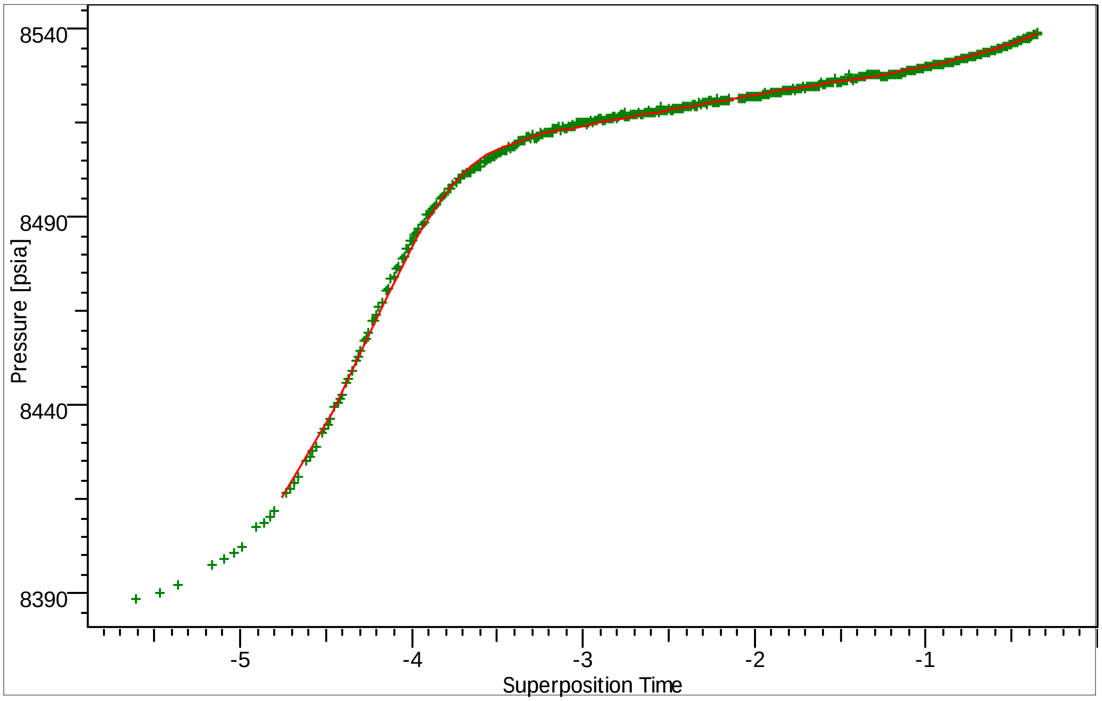

Figure 5.8: Semi-Log Graph of Pressure Data from Well TW002

The pressure data was matched with the homogeneous reservoir model and the skin was determined to be 11.2. The average permeability was found to be 2230 md and represents an equivalent value for the fracture/matrix system of the naturally fractured reservoir. At the late time region of the pressure response, a linear flow pattern is observed. From computation of the late time data, no-flow parallel boundaries were observed to be a distance of 2010 ft south and 1950 ft north of the well. The well is considered to be centered slightly unevenly in a channel. The results of the well test analysis are shown is Table 5.1.

`

Table 5.1: Pressure Transient Test Results for Well TW002

Selected Model		
Model Option	Standard Model	
Well	Vertical	
Reservoir	Homogeneous	
Boundary	Parallel faults	
Main Model Parameters		
TMatch	525	[hr]-1
PMatch	0.146	[psia]-1
C	0.014	bbl/psi
Total Skin	11.2	--
k.h, total	95000	md.ft
k, average	2230	md
Pi	8553.01	psia
Model Parameters		
Well & Wellbore parameters (Tested well)		
C	0.014	bbl/psi
Skin	11.2	--
Boundary parameters		
S - No flow	1950	ft
N - No flow	2010	ft
PVT Parameters		
Volume Factor B	1	B/STB
Viscosity	3.83	cp
Porosity	0.06	
Total Compressibility. ct	1.07E-05	psi-1
Form. Compressibility.	3.00E-06	psi-1

The porosity of the well of the formation around the well TW002 was determined to be about 6% from core analysis and well logs. Since the porosity of the rock matrix is so low, the homogeneous behavior observed in the pressure test analysis is interpreted to be because the fluids in the reservoir are contained mainly in the connected vug and fracture system and fluid flow occurs radially with sufficiently homogeneity.

This seemingly straightforward interpretation is not consistent with mapped boundaries for the drainage area for this well. To produce more reasonable distances to boundary

`

limits, the porosity was adjusted to 30%. The porosity adjustment may be attributed to natural fractures and vugs distributed uniformly enough to result in apparently homogeneous flow behavior.

`

CHAPTER VI

SINGLE FRACTURE MODEL

6.1 Introduction

When a well is drilled such that it intersects a major natural fracture or is producing near a major natural fracture or conductive fault, high flow rates may occur. The two cases are illustrated in Figure 6.1. This major extended natural fracture or conductive fault can be detected by well test analysis. In the case of vuggy naturally fractured reservoirs, any large elongated opening connected or very near to the well that allows for increased secondary porosity in terms of increased fluid storativity or fluid mobility or both may be due to disconnected vugs, connected vugs, channels, major fractures, conductive faults or caves and would have a similar pressure response. The major fracture could act as a channel to drain reservoir fluid from regions located away from the wellbore. In some cases the fracture reaches an aquifer and water is produced.

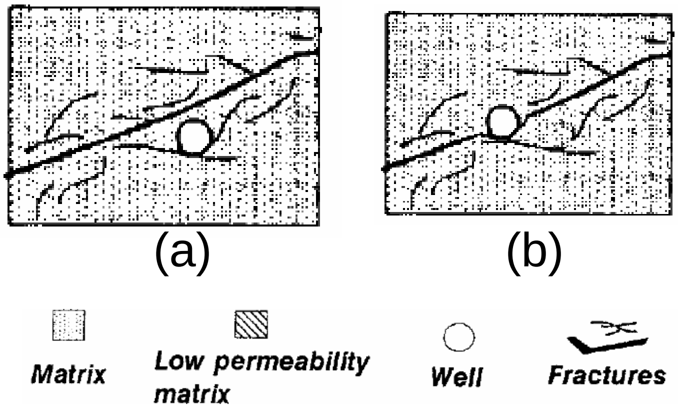

Figure 6.1: Well Producing Next to a Single Fracture (a) and Well Intersecting a Single Fracture (b)

`

Four distinct flow patterns (Figure 6.2) may occur in the fracture and formation around the well. These flow patterns include fracture linear flow, formation linear, bilinear flow and pseudoradial flow. Fracture linear flow is short-lived and is usually masked by wellbore storage. Bilinear flow occurs when the fluid in the fracture flows linearly into the wellbore while the fluid around the fracture flows linearly into the fracture. It is characterized by a quarter slope straight line on the derivative curve. Fracture linear flow occur when fluid flow into the well occurs linearly through the fracture.

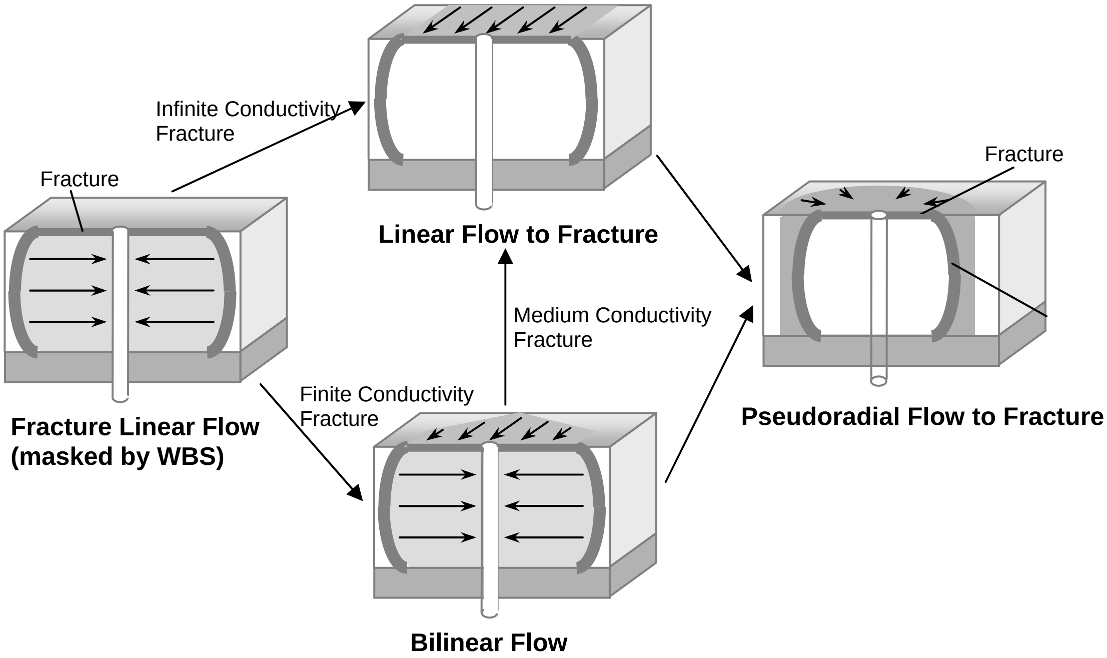
Infinite Conductivity
Fracture
Fracture
Linear Flow to Fracture
Fracture
Medium Conductivity
Fracture
Finite Conductivity
Fracture
Fracture Linear Flow
(masked by WBS)
Pseudoradial Flow to Fracture
Bilinear Flow

Figure 6.2: Flow Patterns Associated with Single Fracture Model (after Ehlig-Economides[25])

`

6.2 Well Producing Next to a Single Major Fracture

The case of a well producing next to a single infinitely conductive fracture is modeled numerically using the Ecrin® software in Figure 6.3 and Figure 6.4. In this case, after the wellbore storage effect, there is a radial flow period characterized by a horizontal straight line. After the radial flow, there is a transition period in which the well behaves as if it were located near a constant pressure boundary (characterized by a -1 slope). Finally the system reaches a bilinear flow period represented by a one-quarter slope straight line in the derivative.

It should be noted that the pressure transient derivative behavior is similar to a pseudosteady state dual porosity model. The flow system is characterized by the formation flow capacity, kh, fracture half-length, x_f and fracture conductivity, $k_f b_f$, and the distance between the well and the fracture, d_f. The model parameters are provided in Table 6.1.

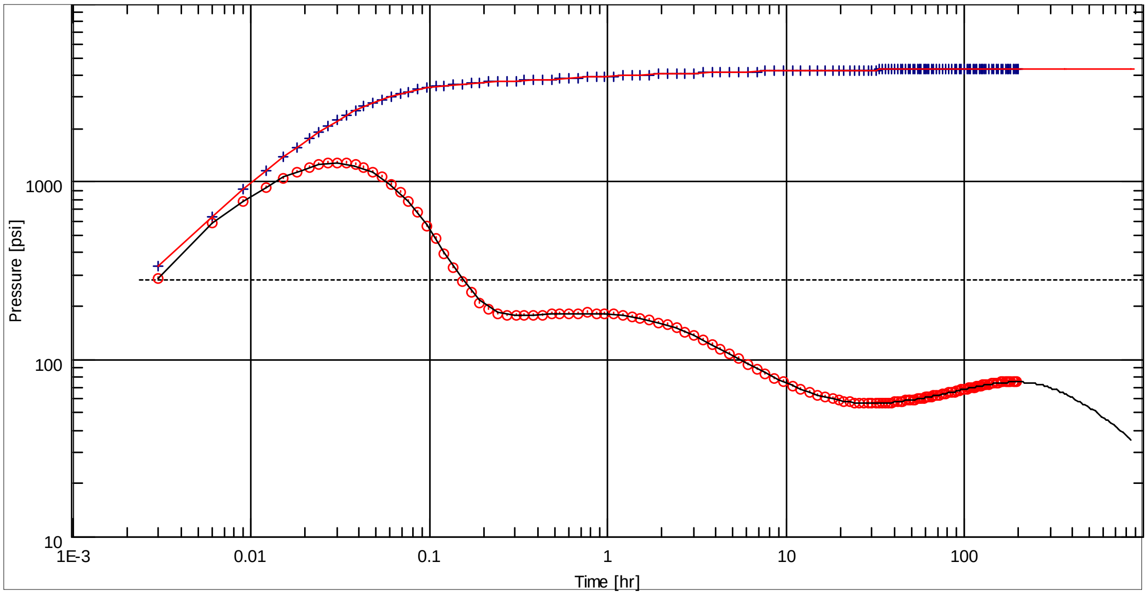

Figure 6.3: Numerical Model of Well Near a Single Major Fracture

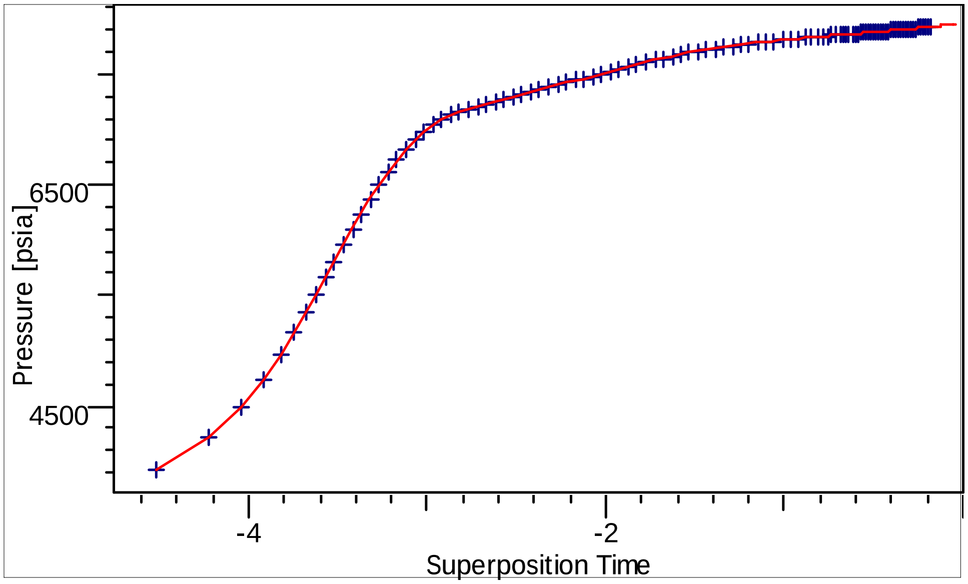

Figure 6.4: Semi-Log Graph of Well Next to Single Major Fracture

`

Table 6.1: Numerical Modeling Results for Well Near a Major Fracture

Test Parameters		
Test Type	Standard	
Fluid Type	Oil	
Rw	0.3	Ft
h	30	Ft
Phi	0.1	--
Selected Model		
Model Option	Numerical	
Well	Fracture - Infinite conductivity	
Reservoir	Homogeneous	
Boundary	Polygonal, No flow	
Top/Bottom	No flow/No flow	
Main Model Parameters		
TMatch	201	[hr]-1
PMatch	0.00177	[psia]-1
C	0.00147	bbl/psi
Total Skin	0.151	--
k.h, total	1000	md.ft
k, average	33.3	md
Pi	8000	psia
Well & Wellbore parameters (Tested well)		
C	0.00147	bbl/psi
Skin	6	--
Geometrical Skin	-5.85	--
Xf	209.713	ft
Well & Wellbore parameters (Well#3)		
Xf	7991.29	ft
Reservoir & Boundary parameters		
Pi	8000	psia
k.h	1000	md.ft
k	33.3	md
Pi	User Imposed	
Module Type	Pseudo Radial	
RMin	1	ft
RMax	2086.94	ft
N Theta	12	--
PVT Parameters		
Volume Factor B	1	B/STB
Viscosity	1	cp
Total Compr. ct	3.00E-06	psi-1
Form. compr.	3.00E-06	psi-1

`

Abbazadeh and Cinco-Ley[26,27] discuss this situation extensively and provide a set of type curves that can be used to analyze the case.

6.3 Wells Intersecting a Major Natural Fracture

In the case where a test well intersects a major natural fracture in the formation, the well would act as though it had been hydraulically fractured. The flow system is characterized by the formation flow capacity, kh , fracture half-length, x_f and fracture conductivity, $k_f b_f$. Figure 6.5 shows a log-log plot of an analytical model of a well intersecting a major natural fracture of half-length ranging from 400 ft to 800 ft. The fracture is infinitely conductive and causes a linear flow pattern in the reservoir.

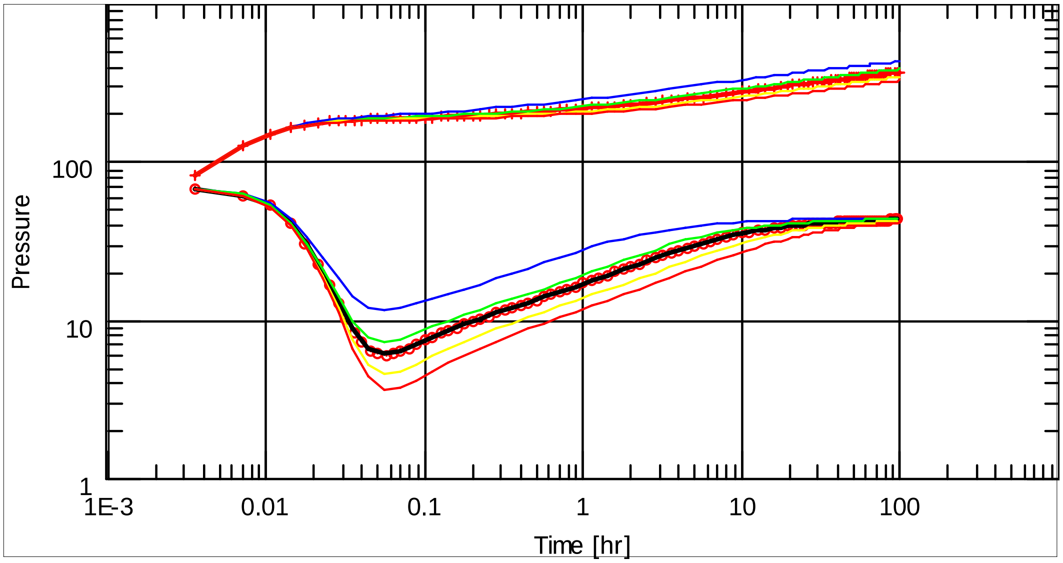

Figure 6.5: Well Penetrating a Major Fracture Sensitivity to Fracture Half-Length

6.4 Field Case Study

A 400 hour build-up was performed on test well TW102. Commercial well test software, Ecrin® was used for computation, regression and test analysis. Figure 6.6 shows the plot of the pressure and pressure derivative against time on a logarithmic scale. The pressure and input data was corrected for scatter and inconsistencies. This was done by synchronizing initial start time of the buildup pressure data by adjusting it to match the time at the start of the pressure buildup.

An examination of the derivative curve reveals two specific flow regimes: linear flow occurs at the middle time region characterized by a half slope in both the pressure and the pressure derivative curve, infinite acting radial flow occurs next at the late time region characterized by a horizontal straight line in the derivative curve.

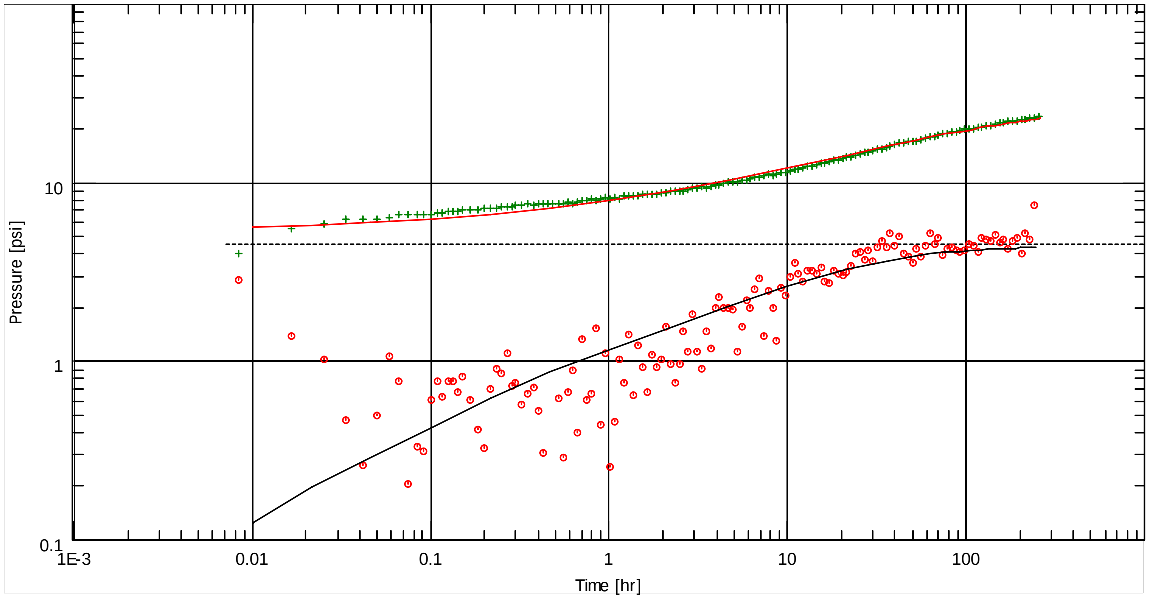

Figure 6.6: Log-Log Pressure and Derivative Curve for Well TW103

`

Table 6.2: Results of the Analysis of Well TW103

Selected Model		
Model Option	Standard Model	
Well	Fracture – Infinite conductivity	
Reservoir	Homogeneous	
Boundary	Infinite	
Main Model Parameters		
Tmatch	0.0283	[hr]-1
Pmatch	0.11	[psia]-1
C	0.0253	bbl/psi
Total Skin	-8.36	--
k.h, total	98300	md.ft
k, average	2500	md
Pi	8476.45	psia
Model Parameters		
Well & Wellbore parameters (Tested well)		
C	0.0253	bbl/psi
Skin	0	--
Geometrical Skin	-8.36	--
Xf	2120	ft
Reservoir & Boundary parameters		
Pi	8476.45	psia
k.h	98300	md.ft
k	2500	md
Derived & Secondary Parameters		
Rinv	10200	ft
Test. Vol.	0.382548	bcf
Delta P (Total Skin)	-75.766	psi
Delta P Ratio (Total Skin)	-2.25776	Fraction

The well is assumed to have been drilled into a major extended natural fracture with fracture half length of 2000 ft. This has a very positive effect on productivity comparative to a hydraulic fracture in a well in a homogeneous reservoir. The results of the analysis are shown in Table 6.2.

`

CHAPTER VII

COMPOSITE RESERVOIR MODEL

7.1 Introduction

Heterogeneities in some naturally fractured reservoirs may be regional. A naturally fractured reservoir can be composed of two regions and these systems are regarded a radial composite reservoir. The radial composite naturally fractured reservoir is illustrated in Figure 7.1. One of the regions can be regarded as a high transmissivity region and the other can be regarded as a low transmissivity region. Productivity in the fractured section of the reservoir would be higher than that of the unfractured reservoir. Pressure transient tests can be used to identify radial composite reservoirs.

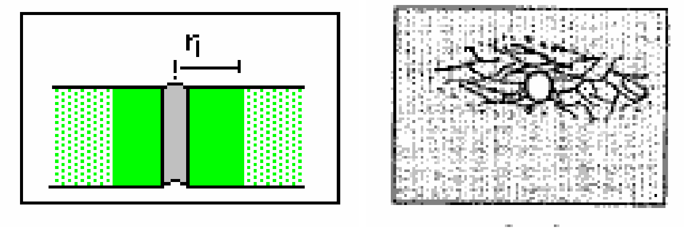

Figure 7.1: Radial Composite Naturally Fractured Reservoirs

A single well test performed in a well drilled into the fractured zone is first affected by the reservoir characteristics of the fractured region then the pressure response is later controlled by the properties of the unfractured zone. The model gives two different permeability values obtained from the two different radial flows observed. The system is therefore characterized by the flow capacity of the fractured region, $(kh)_1$ and that of the unfractured zone, $(kh)_2$, mobility ratio, M, diffusivity ratio, D, and distance to the interface, r_i . The model assumes that the well is at the center of a circular homogeneous zone, communicating with an infinite homogeneous reservoir. The inner and outer zones have different reservoir and/or fluid characteristics. It is also assumed that there is no pressure loss at the interface between the two zones.

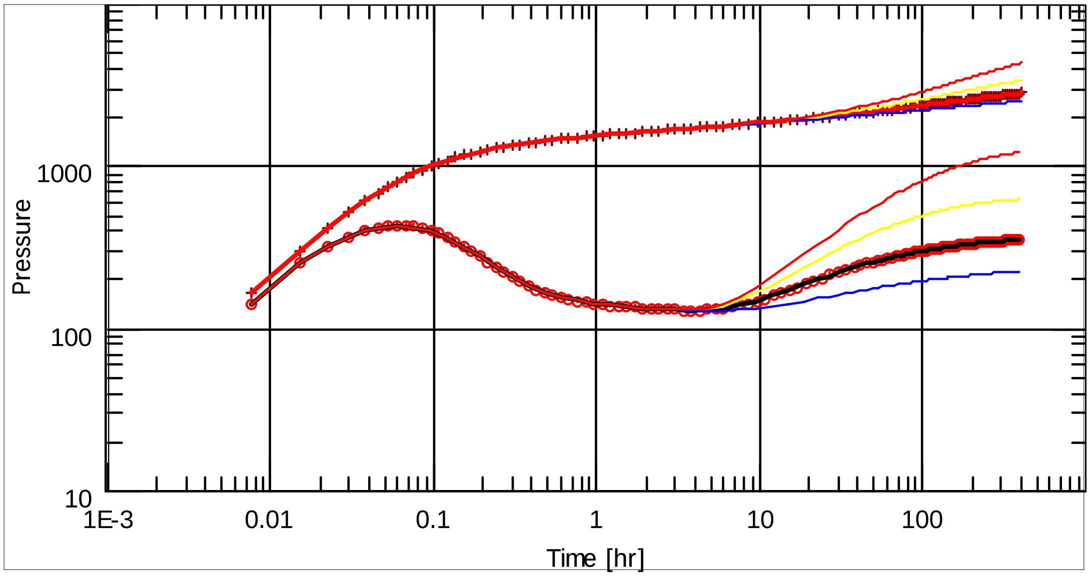

Figure 7.2: Derivative Type Curve of a Radial Composite Model with Varying M

The log – log graph of the pressure derivative shows, at early time, the typical behavior of wellbore storage, followed by a horizontal straight line portion representing a homogeneous radial flow controlled by the inner fractured zone as shown in Figure 7.2. The pressure match should be on the first stabilization. After a transition, the derivative curve rises to a second homogeneous radial flow characterized by a second straight horizontal line, corresponding to the outer unfractured zone. The pressure derivative shows two stabilizations and the time of transition between the two homogeneous flow regimes is a function of r_i and $k / \phi\mu c_t$ for the inner zone. The ratio of the constant derivative levels is equal to the mobility ratio, the shape of the transition between the two homogeneous behaviors is governed by the ratio of the mobility ratio to that of the diffusivity ratio.

7.2 Field Case Study

Well test data obtained from test well TW009 was analyzed using the Ecrin® software. A radial composite match was obtained and the permeability of 1350md was obtained.

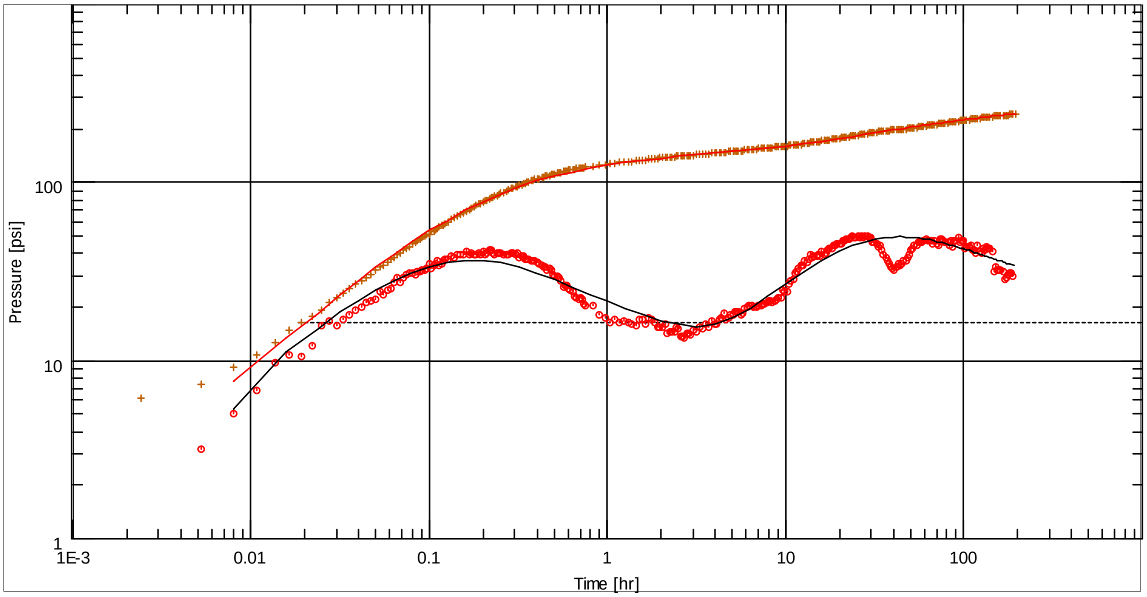

Figure 7.3: Log-Log Pressure and Pressure Derivative Curve for Well TW009

`

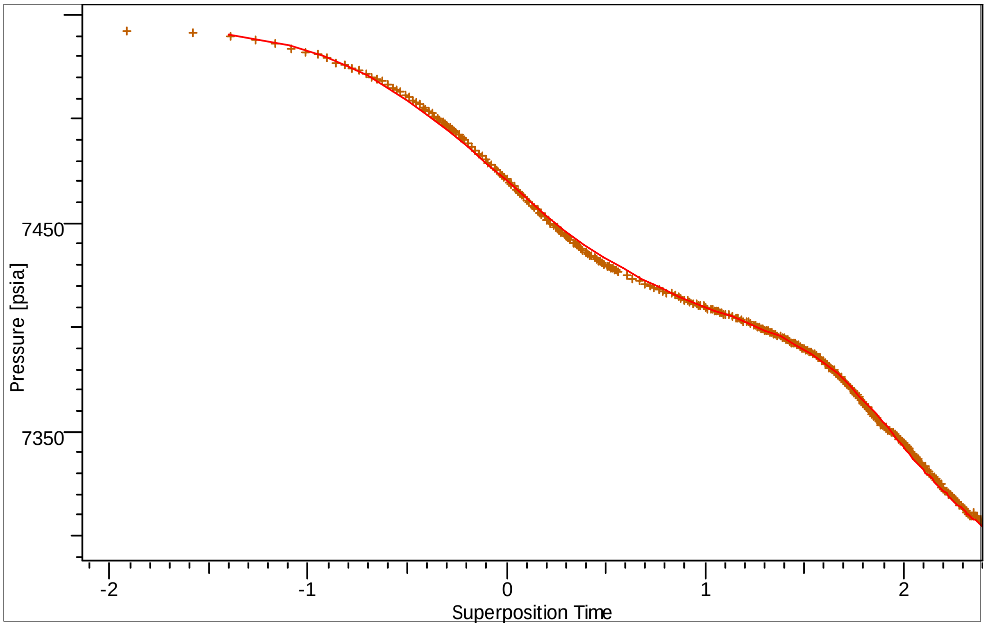

Figure 7.4: Semilog Curve for Well TW009

Figure 7.3 shows the plot of the pressure and pressure derivative against time on a logarithmic scale while Figure 7.4 shows the semi-log plot of the pressure against superposition time. The pressure and input data was corrected for scatter and inconsistencies.

An examination of the derivative curve reveals three specific flow regimes: wellbore storage at the early time region characterized by a unit slope in both the pressure and the pressure derivative curve, infinite acting radial flow at the middle time region characterized by a horizontal straight line in the derivative curve and representing the flow capacity of the fractured zone. The fractured zone has a radius of 1840 ft. The

`

derivative curve later rises to a new homogeneous radial flow level that represents the properties of the unfractured zone. The results of the analysis are shown in Table 6.3.

Table 6.3: Results of the Analysis of Well TW009

Selected Model		
Model Option	Standard Model	
Well	Vertical	
Reservoir	Radial composite	
Boundary	Infinite	
Rw	0.246063	ft
h	65.6168	ft
Phi	0.02	--
Main Model Parameters		
TMatch	27.5	[hr]-1
PMatch	0.0309	[psia]-1
C	0.0353	bbl/psi
Total Skin	-3.94	--
k.h, total	88800	md.ft
k, average	1350	md
Pi	7627.85	psia
Model Parameters		
Well & Wellbore parameters (Tested well)		
C	0.0353	bbl/psi
Skin	-3.94	--
Reservoir & Boundary parameters		
Pi	7627.85	psia
k.h	88800	md.ft
k	1350	md
Ri	1810	ft
M	1.48	--
D	0.0312	--
PVT Parameters		
Volume Factor B	1	B/STB
Viscosity	27	cp
Total Compr. ct	2.76E-06	psi-1
Form. compr.	3.00E-06	psi-1

CHAPTER VIII

DUAL POROSITY MODEL

Double-porosity systems reduce the heterogeneities in the vuggy naturally fractured reservoir such as fractures, vugs, caverns and cavities into essentially two media: a conductive network and storative matrix. The conductive network provides reservoir fluid flow channels while the reservoir fluids are stored in both media. The models proposed to date differ conceptually only in the assumptions made to describe fluid flow in the matrix. The models consider regularly shaped matrix blocks such as cubes, parallelepipeds, cylinders or spheres and assume that fluid transfer between matrix and fractures occur through transient or pseudosteady state conditions. The model is illustrated in Figure 8.1.

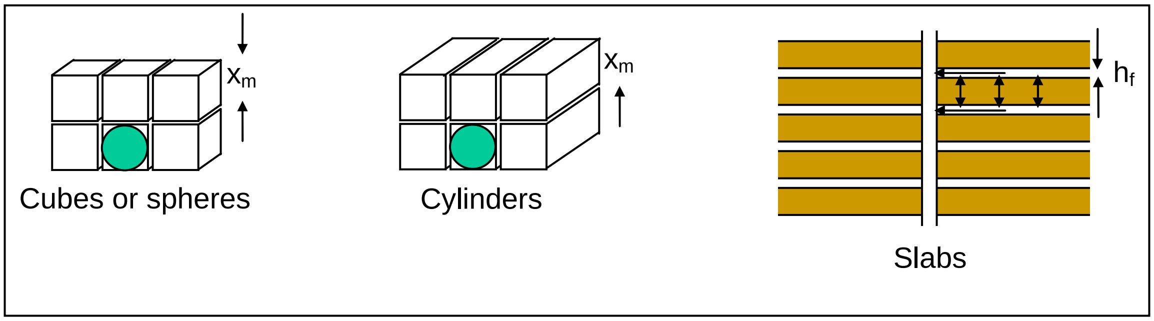

Figure 8.1: Schematics for Dual Porosity Models

The models are characterized by the same parameters used to characterize homogeneous (single porosity) reservoirs with two additional parameters[2], the storativity ratio ω and the interporosity flow coefficient, λ. These two parameters, ω and λ, are usually determined from pressure-transient analysis. The storativity ratio, ω determines the

`

amount of fluid stored in the fracture system compared to the total fluid in the reservoir (matrix and fracture). The storativity ratio is defined as:

$$w = \frac{\phi_f c_{tf}}{\phi_f c_{tf} + \phi_m c_{tm}} \qquad \text{..8.1}$$

where ϕ is porosity and c_t is total compressibility. Subscripts *f* and *m* represent fracture and matrix, respectively.

The interporosity flow coefficient determines the fluid exchange interaction between matrix system and fracture system. High value of λ indicates the fluid easily flow from the matrix to the fracture system while low values of λ indicate the opposite. The interporosity flow coefficient λ is defined as:

$$\lambda = \alpha r^2{}_w \frac{k_m}{k_f} \qquad \text{..................................8.2}$$

where k_m is the permeability of the matrix, k_f is the permeability of the fracture network and α is a system geometric factor that depends on the shape of the matrix blocks and has a dimension of length.

$$\alpha = \frac{A}{xV} \qquad \text{..8.3}$$

`

where A is the surface area of matrix blocks, V is the volume of matrix blocks, and x is the characteristic length.

For uniformly spaced fractures,

$$\alpha = 4n(n+2)/x^2 \qquad \text{8.4}$$

where n = number of normal sets of fractures

For squares and spheres, n = 3, and

$$\lambda = \frac{60}{x_m{}^2}\frac{k_m}{k_f}r_w{}^2 \qquad \text{8.5}$$

where x_m is the length of cube side of sphere diameter

For cylinders, n = 2 and

$$\lambda = \frac{32}{x_m{}^2}\frac{k_m}{k_f}r_w{}^2 \qquad \text{8.6}$$

where x_m is the length of square side, or diameter of circular cylinder

For slabs, n = 1 and

$$\lambda = \frac{12}{h_f{}^2}\frac{k_m}{k_f}r_w{}^2 \qquad \text{8.7}$$

where h_f is the fracture thickness.

`

8.1 Double-Porosity Model with Pseudosteady-State Interporosity Flow

In this model, the flow from the matrix blocks to the fracture system is assumed to be under pseudosteady state conditions. All reservoir fluid production is assumed to occur through the fracture system only and radial flow occurs in the fracture system. This matrix-fracture model is identical to the one proposed by Warren and Root[1]. The modified diffusivity equation becomes:

$$\frac{1}{r}\frac{\partial}{\partial r}\left(r\frac{k_f}{\mu}\frac{\partial p_f}{\partial r}\right)=\phi_f c_{t_f}\frac{\partial p_f}{\partial t}+\phi_m c_{t_m}\frac{\partial \overline{p}_m}{\partial t}\ \ldots\ldots\ldots\ldots\ldots\ldots 8.8$$

Dimensionless variables for pressure and time are defined as:

$$p_{wD}=\frac{k_f h\Delta p}{\alpha_p qB\mu}\ \ldots\ldots\ldots\ldots\ldots\ldots 8.9$$

$$t_D=\frac{\alpha_f k_f t}{\left(\phi_f c_{tf}+\phi_m c_{tm}\right)\mu r_w^{\ 2}}\ \ldots\ldots\ldots\ldots\ldots\ldots 8.10$$

The diffusivity equation in dimensionless variables becomes:

$$\frac{1}{r_D}\frac{\partial}{\partial r_D}\left(\frac{\partial p_{Df}}{\partial r_D}\right)=\omega\frac{\partial p_{Df}}{\partial t}+(1-\omega)\frac{\partial \overline{p}_{Dm}}{\partial t}\ \ldots\ldots\ldots\ldots\ldots\ldots 8.11$$

The partial differential equation that describes the pseudosteady-state interporosity flow in the matrix is given by[25]:

$$\phi_m c_{t_m} V_m\frac{\partial \overline{p}_m}{\partial t}=\frac{k_m}{\mu}A_m(\overline{p}_m-p_f)\ \ldots\ldots\ldots\ldots\ldots\ldots 8.12$$

In dimensionless form, it becomes

$$(1-\omega)\frac{\partial \overline{p}_{Dm}}{\partial t} = \lambda(\overline{p}_{Dm} - p_{Df}) \quad \text{..8.13}$$

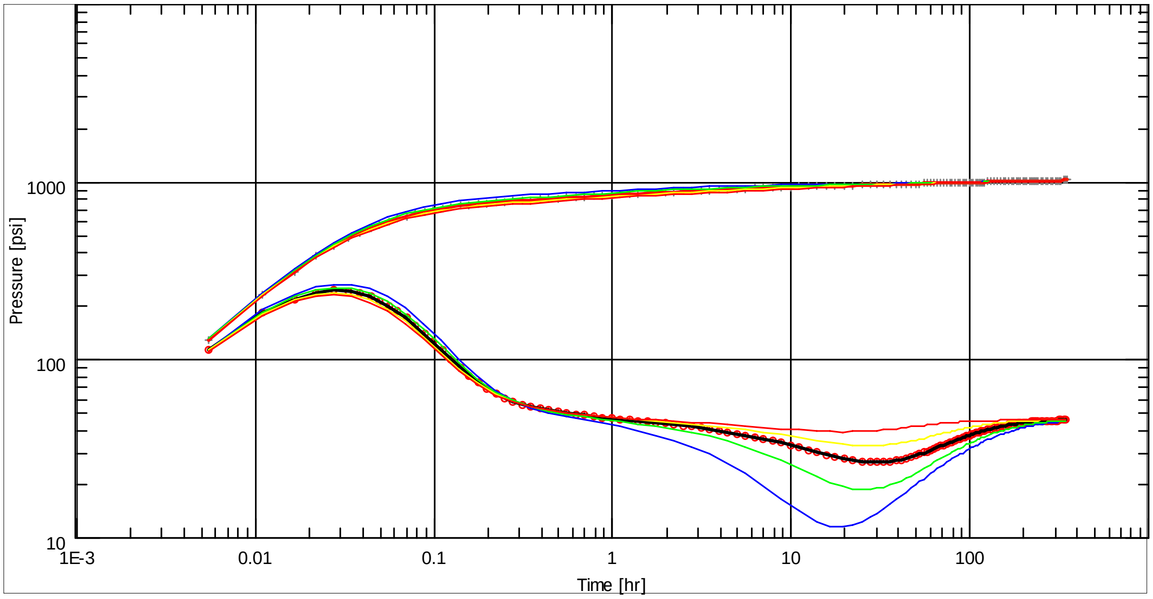

Figure 8.2: Typical Behavior of Dual Porosity Reservoir with Varying Omega Values

Figure 8.2 presents a typical behavior for a single well test. At the earliest times, the reservoir behaves like a homogeneous reservoir with all the fluid originating from the fracture system. The wellbore storage effects are seen at the early stage of the derivative curve on a log-log scale. After a transition period, a horizontal line signifying radial flow develops. This radial flow regime is due to homogeneous fluid flow from the fractures. During intermediate times, the rock matrix interacts with the fractures and begins to produce into the fractures. At this point, a characteristic V-shaped valley can be seen on the curve. This dip below the homogeneous reservoir curve is the most notable feature of

`

naturally fractured reservoir. The curve dipping downward is characteristic of a parameter $\lambda C_D / \omega(1-\omega)$ and the rise back to homogeneous behavior is characterized by $\lambda C_D /(1-\omega)$. The depth of the "valley" is a function of the storativity ratio, ω, while the time of transition is a function of the interporosity ratio, λ.

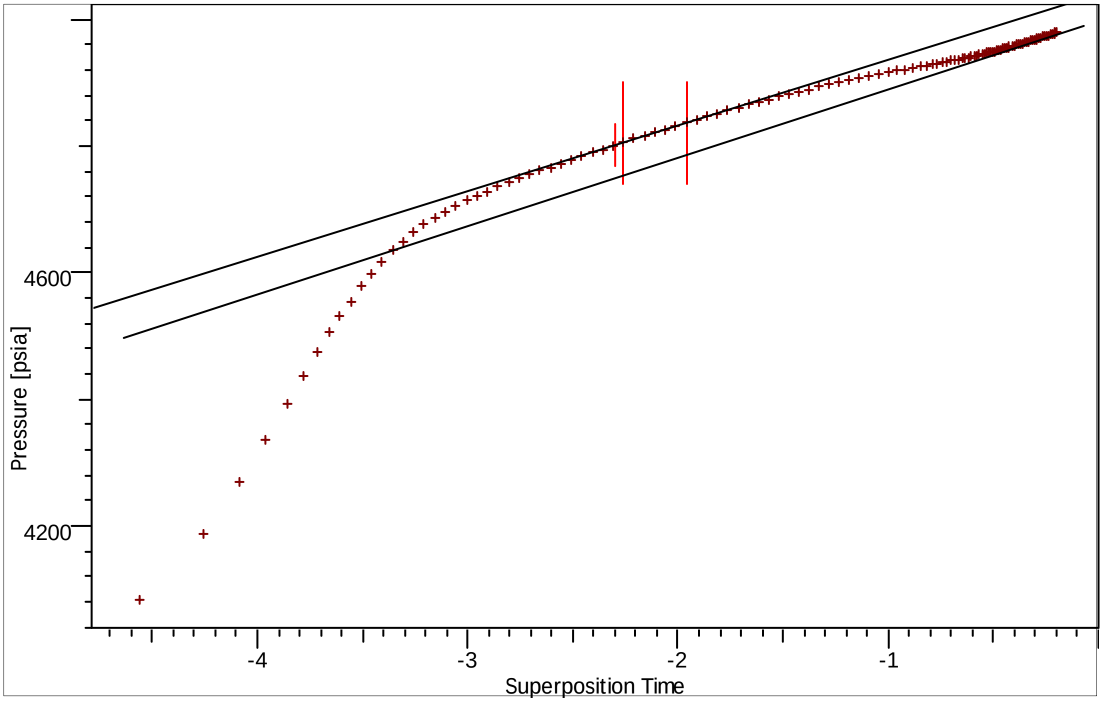

Figure 8.3: Typical Behavior of Dual Porosity Reservoir on Semi-Log plot

When the matrix and fracture fluid transfer has reached pseudosteady state flow conditions, a horizontal straight line representing homogeneous radial flow from the total system (matrix + fracture) is observed again on the derivative curve. The semilog graph in Figure 8.3 shows two parallel straight lines which represent the fracture dominated flow period and the total reservoir (fracture + matrix) dominated flow period.

The permeability of the total system is estimated from the slope of the semilog straight lines while the skin factor is calculated from the first of the two parallel straight lines. Dual porosity behavior needs to be confirmed with geologic information and reservoir performance.

8.2 Field Case Study

A 30 hour build-up was performed on test well TW004. Figures 8.4 and 8.5 shows the plot of the pressure and pressure derivative against time on a logarithmic scale. The pressure and input data was corrected for scatter and inconsistencies.

An examination of the derivative curve reveals three specific flow regimes: wellbore storage at the early time region characterized by a unit slope in both the pressure and the pressure derivative curve, infinite acting radial flow at the middle time region characterized by a horizontal straight line in the derivative curve. The formation was determined to have an average permeability of 3420 md. There is a characteristic valley in the radial flow behavior that suggests pseudosteady state dual porosity behavior. In the late time period, the derivative curve rising with a half slope indicating the possible presence of 2 parallel no-flow boundaries in the late time region. The results of the analysis are shown in Table 8.1.

`

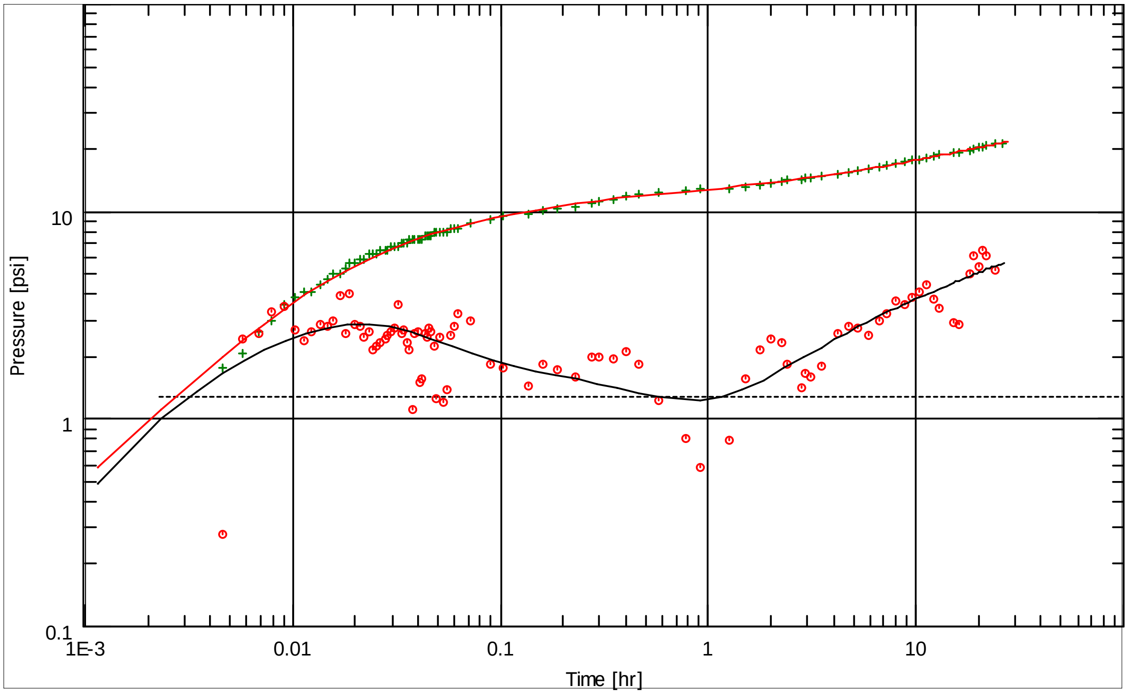

Figure 8.4: Log-Log Pressure and Pressure Derivative Curve for Well TW004

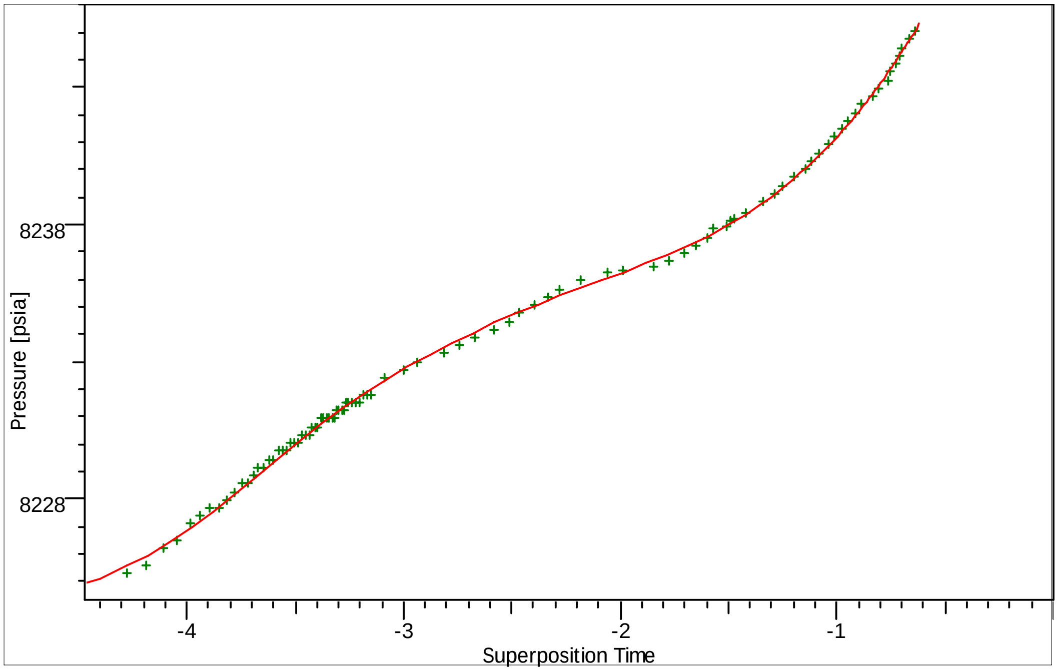

Figure 8.5: Semi-Log Curve for Well TW004

`

Table 8.1: Pressure Transient Analysis Solution of Well TW004

Test Parameters		
Test Type	Standard	
Fluid Type	Oil	
Rate Type	Surface rates	
Rw	0.246063	ft
H	226.378	ft
Phi	0.019	--
Selected Model		
Model Option	Standard Model	
Well	Vertical	
Reservoir	Two porosity PSS	
Boundary	Parallel faults	
Top/Bottom	No flow/No flow	
Main Model Parameters		
TMatch	219	[hr]-1
PMatch	0.391	[psia]-1
C	0.0853	bbl/psi
Total Skin	-3.65	--
k.h, total	7.77E+05	md.ft
k, average	3430	md
Pi	8263.55	psia
Model Parameters		
Well & Wellbore parameters (Tested well)		
C	0.0853	bbl/psi
Skin	-3.65	--
Reservoir & Boundary parameters		
Pi	8263.55	psia
k.h	7.77E+05	md.ft
k	3430	md
Omega	0.223	--
Lambda	1.00E-07	--
S - No flow	413	ft
N - No flow	936	ft
PVT Parameters		
Volume Factor B	1	B/STB
Viscosity	12.28	cp
Total Compr. ct	1.56E-05	psi-1

CHAPTER IX

TRIPLE POROSITY MODEL

The triple porosity model is an extension of the double porosity model. In the triple porosity model, three mediums are considered: fracture system, rock matrix system and the vug/cavity system. The triple porosity model is based on the assumption that the fracture system interacts with both the matrix system and the vug system. The matrix system provides primary porosity while the vug system provides a high secondary porosity comparable or greater than that of the matrix system.

The matrix and vug system provide storage space for the reservoir fluid but have no direct contribution to the global fluid flow and transport. Similar to the dual porosity model, fluid flow into the well occurs only through the fracture system. This model is known as a triple porosity/ single permeability model.

The assumptions of the model are:

- The reservoir is of uniform thickness
- slightly compressible fluid
- Fluid flow into the well is radial and occurs only through the fracture system
- The properties such as permeability, initial porosity and compressibility within each porosity system is constant

`

9.1 Mathematical Model

The differential equation for the fractures can be written, using dimensionless variables as:

$$\frac{1}{r_D}\frac{\partial}{\partial r_D}\left(r_D\frac{\partial p_{Df}}{\partial r_D}\right)+\lambda_{mf}\left(p_{Dm}-p_{Df}\right)+\lambda_{vf}\left(p_{Dv}-p_{Df}\right)=\omega_f\frac{\partial p_{Df}}{\partial t_D}\quad\ldots\ldots\text{..9.1}$$

For the matrix blocks, the equation is

$$-\lambda_{mv}\left(p_{Dm}-p_{Dv}\right)--\lambda_{mf}\left(p_{Dm}-p_{Df}\right)=\left(1-\omega_f-\omega_v\right)\frac{\partial p_{Dm}}{dt_D}\quad\ldots\ldots\ldots\ldots\text{..9.2}$$

And for vugs, the equation is as follows:

$$\lambda_{mv}\left(p_{Dm}-p_{Dv}\right)--\lambda_{vf}\left(p_{Dv}-p_{Df}\right)=\omega_v\frac{\partial p_{Dm}}{dt_D}\quad\ldots\ldots\ldots\ldots\ldots\ldots\ldots\text{..9.3}$$

Where the dimensionless variables are given by

$$p_{Dj}=\frac{2\pi k_f h(p_i-p_j)}{q\mu B_o}\quad\ldots\ldots\ldots\ldots\ldots\ldots\ldots\ldots\ldots\ldots\text{9.4}$$

Where j represents fractures or vugs as needed.

$$t_D=\frac{k_f t}{\mu r_w{}^2\left(\phi_f c_{tf}+\phi_m c_{tm}+\phi_v c_{tv}\right)}\quad\ldots\ldots\ldots\ldots\ldots\ldots\ldots\ldots\text{9.5}$$

The interporosity factors are defined as

$$\lambda_{mf}=\frac{\alpha_{mf}k_m r_w{}^2}{k_f}\quad\ldots\ldots\ldots\ldots\ldots\ldots\ldots\ldots\ldots\ldots\text{..9.6}$$

$$\lambda_{mv}=\frac{\alpha_{mv}k_m r_w{}^2}{k_f}\quad\ldots\ldots\ldots\ldots\ldots\ldots\ldots\ldots\ldots\ldots\ldots\text{9.7}$$

$$\lambda_{vf} = \frac{\alpha_{vf} k_{vf} r_w^{\ 2}}{k_f} \qquad \text{9.8}$$

Where α_{ij} is the interporosity flow shape factor between medium i and j.

The storativity ratios for fractures and vugs are given, respectively by

$$\omega_f = \frac{\phi_f c_{tf}}{\left(\phi_f c_{tf} + \phi_m c_{tm} + \phi_v c_{tv}\right)} \qquad \text{9.9}$$

$$\omega_v = \frac{\phi_v c_{tv}}{\left(\phi_f c_{tf} + \phi_m c_{tm} + \phi_v c_{tv}\right)} \qquad \text{9.10}$$

It should be noted that whereas the double porosity model had 2 additional parameters to help describe the heterogeneities in the system, the triple porosity model requires 5 additional parameters to characterize the model.

Figures 9.1 and 9.2 present typical behavior for a single well test showing triple porosity behavior. The pressure and the pressure derivative plot on the logarithmic scale show specific characteristics of this model. The model is easily identified by the presence of two valleys. The wellbore storage effects are seen at the early stage of the derivative curve on a log-log scale, the well bore storage may mask a portion of the heterogeneous reservoir behavior.

At the earliest times, the reservoir behaves like a homogeneous reservoir with all the fluid originating from the fracture system. After a transition period, a horizontal line signifying radial flow develops. This radial flow regime is due to homogeneous fluid flow from the fractures. During intermediate times, one of the storative porosity systems interacts with the fractures and begins to produce into the fractures. A first characteristic “valley” is observed. This could be the matrix or vugs. When the matrix and fracture fluid transfer has reached pseudosteady state flow conditions, a horizontal straight line representing homogeneous radial flow from the matrix and fracture system is observed again on the derivative curve. The second valley occurs as the other storative porosity system unloads into the fracture. When both porosity systems have been active, a final horizontal straight line is formed.

Alternatively, depending on the reservoir, the first valley may represent the transfer from vug to fracture while the second represents the interporosity transfer from the matrix to fracture. The permeability of the total system is estimated from the slope of the semilog straight lines while the skin factor is calculated from the first of the parallel straight lines. Triple porosity behavior needs to be confirmed with geologic information and reservoir performance.

`

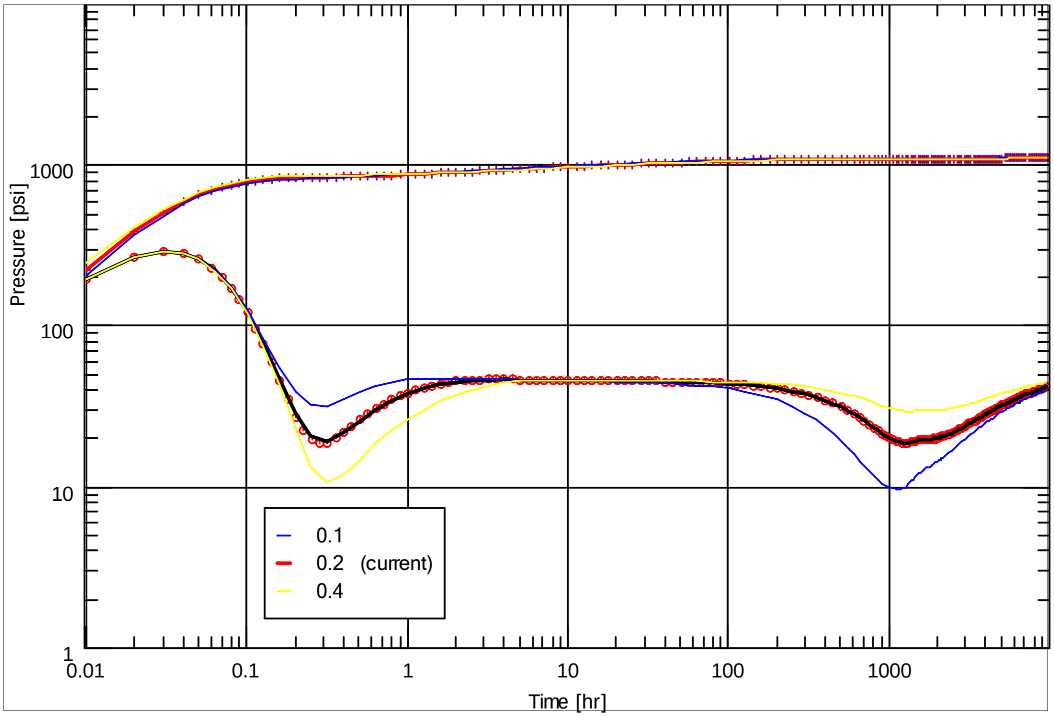

Figure 9.1: Typical Behavior of Triple Porosity Reservoir with Varying Delta Values

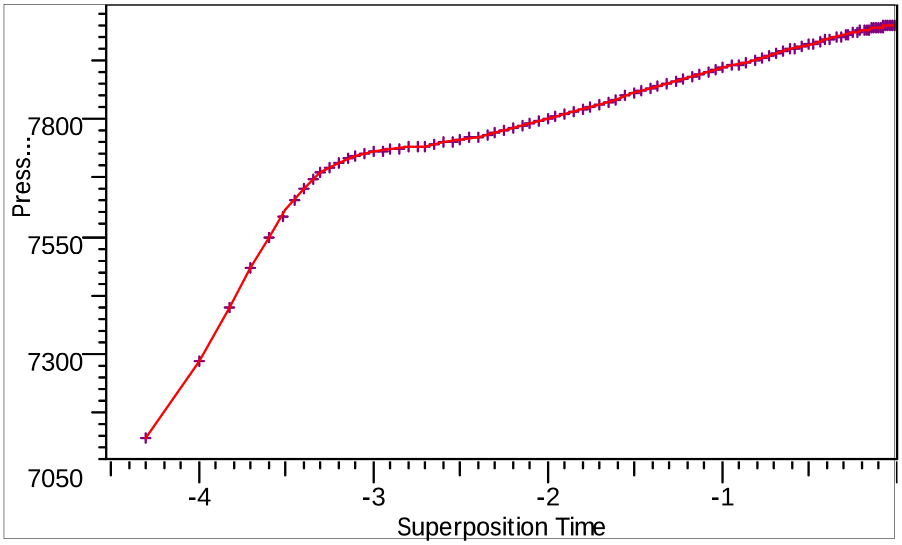

Figure 9.2: Typical Behavior of Triple Porosity Reservoir on Semi-Log Curve

`

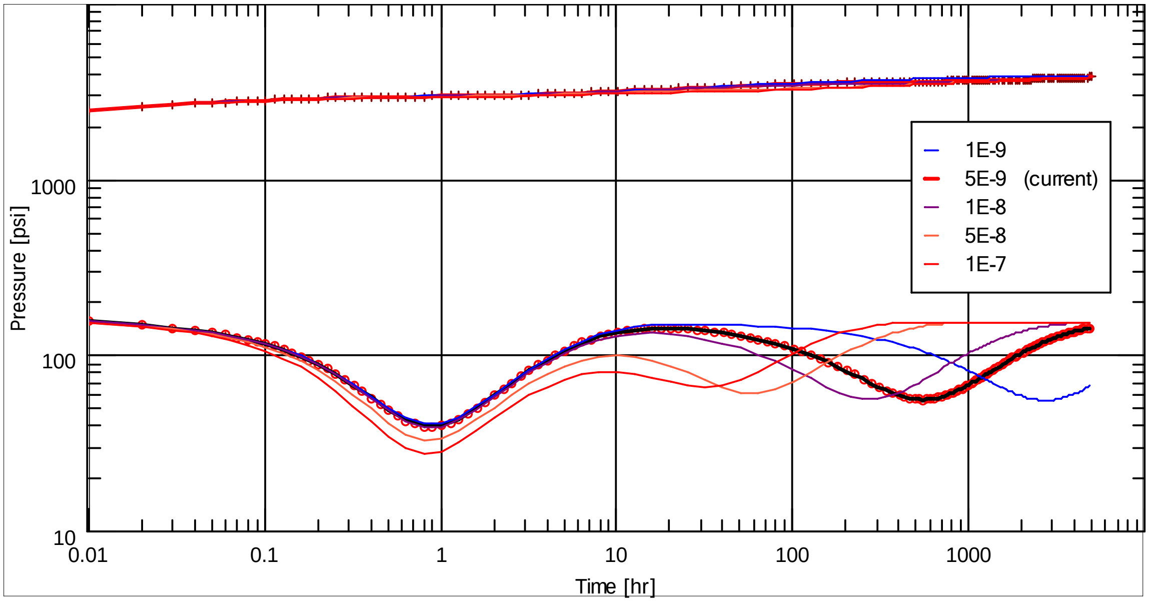

Figure 9.3: Triple Porosity Reservoir with Sensitivity to Matrix Lambda Values

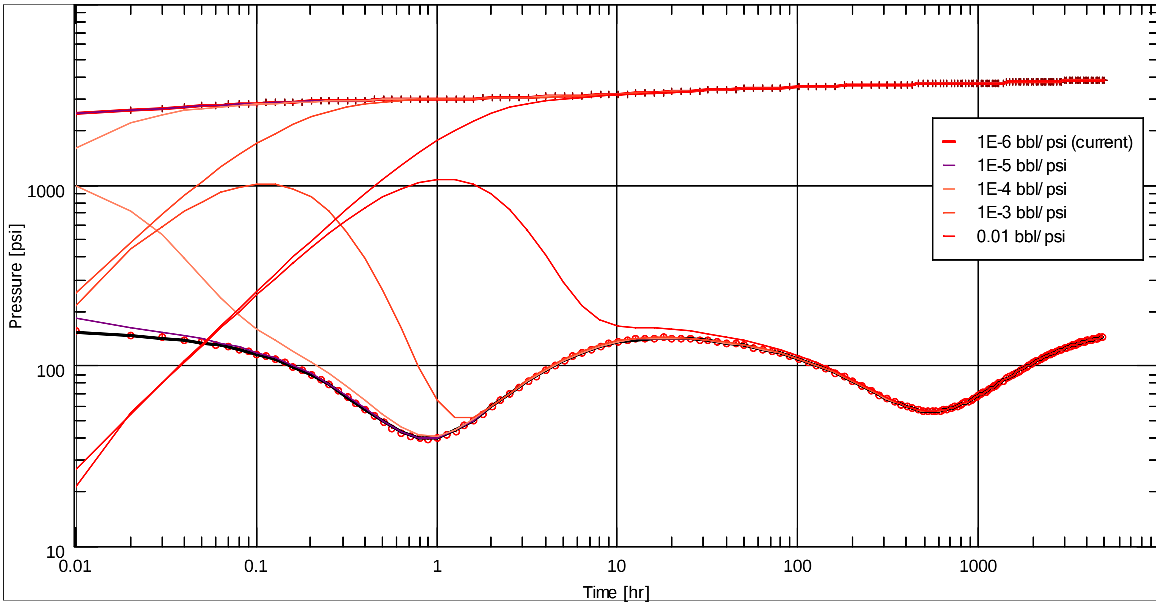

Figure 9.4: Triple Porosity Reservoir with Sensitivity to Wellbore Storage

`

As shown in Figures 9.1 through 9.4, the adequate choice of parameter values may allow the triple porosity behavior to be observed.

The first double-porosity behavior corresponding to the porosity system with the maximum transmissivity value, λ (minimum size), with the classical "valley" on derivative is observed first. Then if the contrast in interporosity flow coefficient is large enough, the second transition corresponding to the second porosity system is observed later in time.

It should be noted that for a constant value of omega, the smaller the delta value, the greater the second valley and the smaller the first one.

9.2 Field Case Study

The match for well TW003 shown in Figures 9.5 and 9.6 exhibit triple porosity behavior with a characteristic double valley. The dip at the end of the derivative data is interpreted as a second valley in the triple porosity model. It is difficult to be sure what the origins of the observed behavior are. If the vugs are highly connected to the fracture system, logically, they would recharge the fractures earlier than the matrix, so the first valley is probably due to vugs. In that case the second valley would be attributed to flow from the matrix to the fractures.

`

Assuming that compressibility for each porosity system is constant, this interpretation indicates that about 85% of the fluid flow originates from the matrix while about 15% of the fluid produced originates from the vugs.

The pressure transient analysis indicates the presence of additional vugular porosity and the vug storativity factor is used to calculate the vug porosity from the triple porosity model. The vug porosity was calculated to be 0.02 and this therefore increases the total porosity from 0.15 to 0.17. This increase in total porosity would ultimately account for an increase in the estimated reserves. The results of the analysis of the well is shown in Table 9.1.

It can be noticed that the well would have to be shut-in for over 42 days in order to observe the rise out of the second valley of the triple porosity reservoir model in the pressure build-up derivative curve. Authorization to shut down a producing well for an extended length of time is not easily obtainable and is discouraged because of the financial implications of lost production during the shut in period.

`

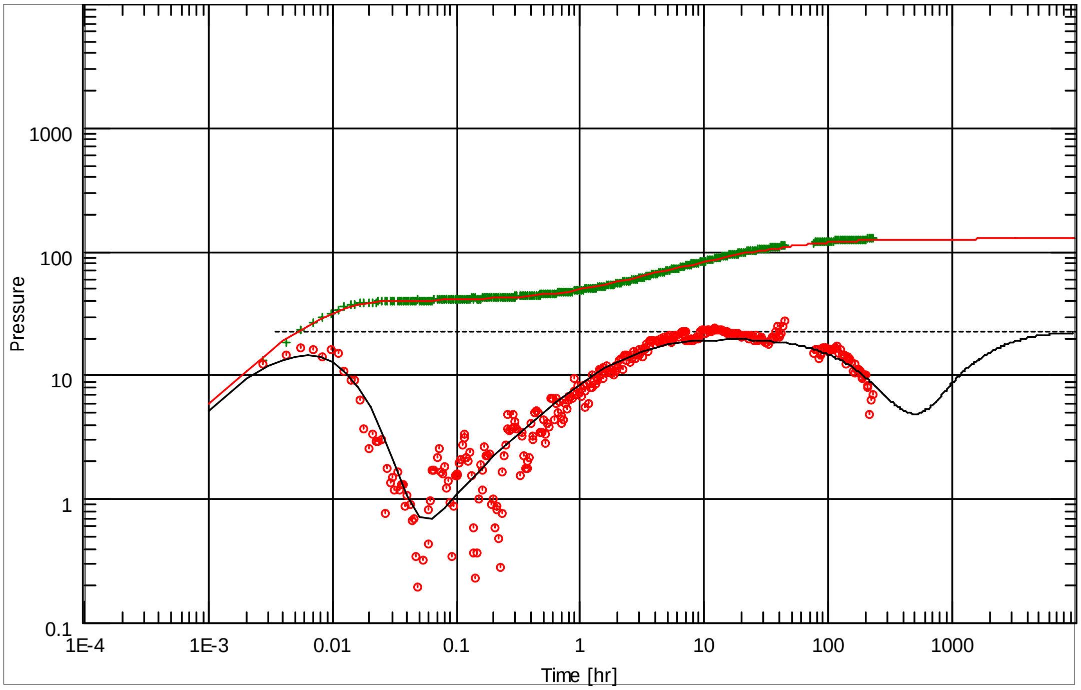

Figure 9.5: Log-log Pressure and Pressure Derivative Curve for Well TW303

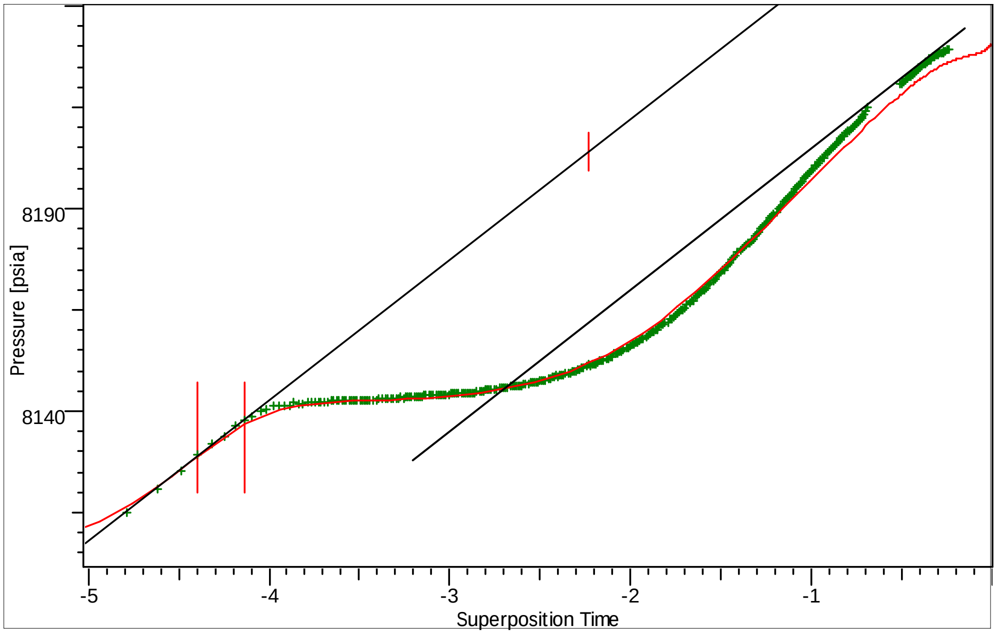

Figure 9.6: Semi-Log Curve for Well TW303

.

`

Table 9.1: Results of the Analysis of Well TW303

Test Parameters		
Test Type	Standard	
Fluid Type	Oil	
Rate Type	Surface rates	
Rw	0.244792	ft
h	73.8189	ft
Phi	0.15	--
Selected Model		
Model Option	External model	
Main Model Parameters		
TMatch	142	[hr]-1
PMatch	0.0224	[psia]-1
C	0.0196	bbl/psi
k.h, total	13600	md.ft
k, average	184	md
Pi	8230.8	psia
Model Parameters		
Well & Wellbore parameters (Tested well)		
C	0.0196	bbl/psi
Reservoir & Boundary parameters		
Pi	8230.8	psia
k.h	13600	md.ft
k	184	md
Skin	-7.36018	--
Omega	4.31E-39	--
Delta1	0.1437	--
Lambda1	2.00E-07	--
Lambda2	1.50E-09	--
Derived & Secondary Parameters		
Delta Q	1510	STB/D
P @ dt=0	8100	psia
Rinv	5290	ft
Test. Vol.	0.973518	bcf
k / mu	128	md/cp
PVT Parameters		
Volume Factor B	1.98	B/STB
Viscosity	1.44	cp
Total Compr. ct	5.94E-06	psi-1
Form. compr.	3.00E-06	psi-1

`

The complex characteristics of the carbonate reservoir and the short testing time allow for the well test data to have a good match with various models. Well TW303 can also be fitted by the dual-porosity model with a constant pressure boundary shown in Figure 9.7, and the radial composite model with dual porosity in Figure 9.8 can also match the transient data.

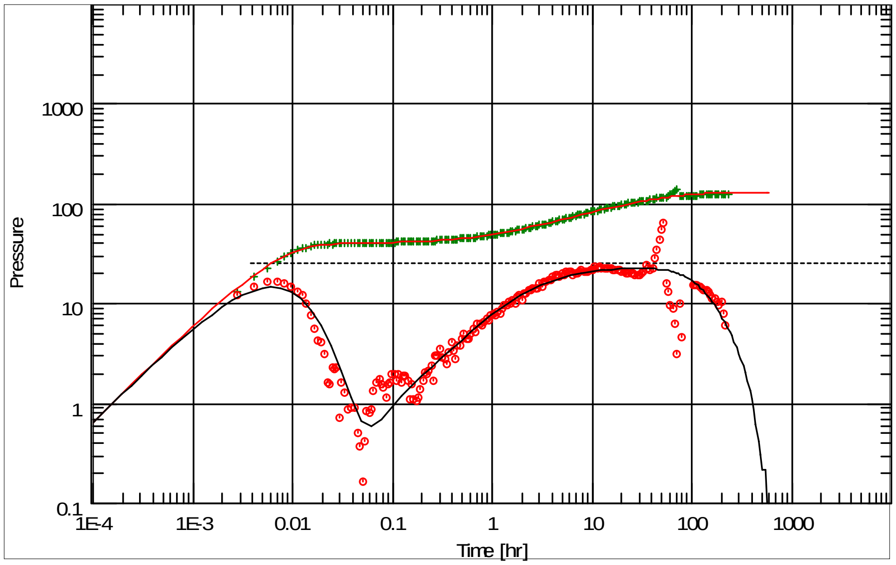

Figure 9.7: Dual-Porosity with Closure Boundary Match for Well TW303

Lack of evidence of a sealing boundaries close enough to the well on the geologic map to account for a closure in the reservoir system could discourage this interpretation. It should be noticed that the double and triple porosity models give similar estimates for the reservoir (fracture system) permeability. However this interpretation implies the

`

quantification of the reservoir while the triple porosity interpretation sees no limit to the well drainage area.

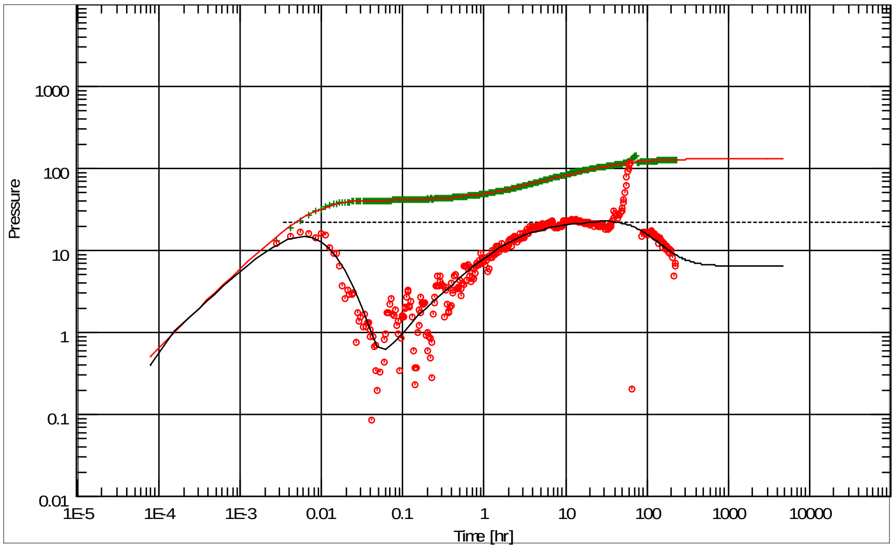

Figure 9.8: Radial Composite Match for Well TW303

The radial composite model assumes that the dip at the end of the derivative curve of the Well TW303 data indicates that the curve is attempting to settle at a new infinite acting radial flow level. It is not possible to quantify the permeability of the outer reservoir region, but, from the match in Figure 9.8, it is at least 440 md. . As with the triple porosity case, this interpretation does not quantify the well drainage area.

Further information obtained from drilling data, production data, core samples and well logs is required to select the model that gives the best interpretation of transient behavior.

`

CHAPTER X

FUTURE MODELS

A few of the analyses could not be classified into the five responses mentioned already and appear to require new models not available in commercial pressure transient test analysis software. In some cases, it was possible to get a match for the data using available models but when the results are compared with information from other sources as well as by experience, it is evident that the models do not properly describe the behavior in the reservoir. For such pressure responses, there is a need to develop new models that provide a more reasonable interpretation for the observed transient behavior.

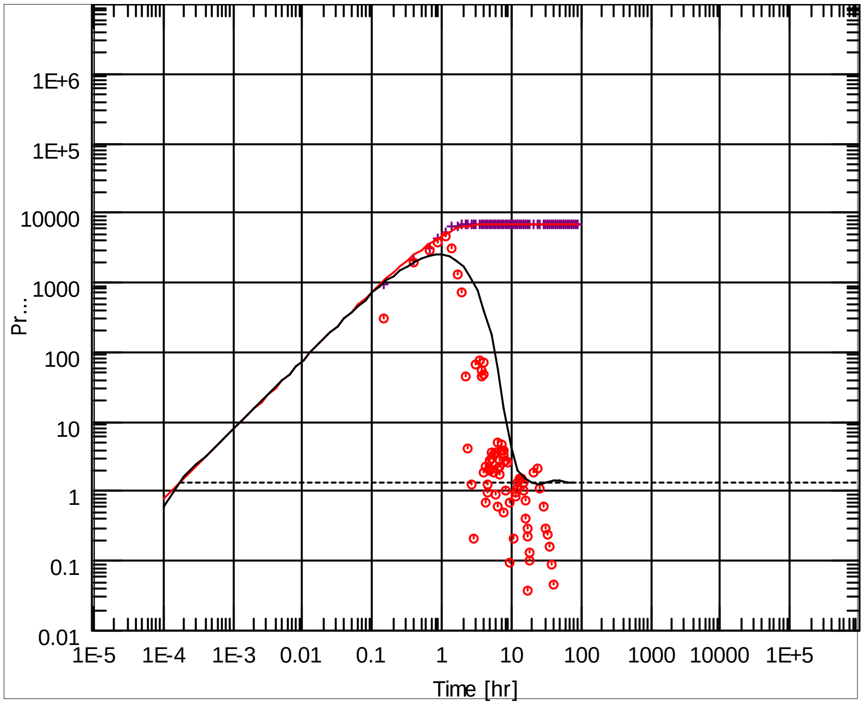

Figure 10.1: Pressure and Derivative Curve of Well TW017

`

Figure 10.1 can be modeled with a homogeneous reservoir model but the apparent value of skin is as high as 2700 and the average permeability is 6000 md. It is suspected that the well has been drilled near a cavern. The results of the analysis of the well TW017 above using available models from commercial software is presented in the Table 10.1.

Table 10.1: Results of the Analysis of Well TW017

Test Parameters		
Test Type	Standard	
Fluid Type	Oil	
Rw	0.246063	ft
h	65.6168	ft
Phi	0.015	--
Model Option	Standard Model	
Well	Vertical	
Reservoir	Homogeneous	
Boundary	Infinite	
Main Model Parameters		
TMatch	2970	[hr]-1
PMatch	0.382	[psia]-1
C	0.00338	bbl/psi
Total Skin	2690	--
k.h, total	3.97E+05	md.ft
k, average	6050	md
Pi	8725.97	psia
Model Parameters		
Well & Wellbore parameters		
C	0.00338	bbl/psi
Skin	2690	--
Reservoir & Boundary parameters		
Pi	8725.97	psia
k.h	3.97E+05	md.ft
k	6050	
PVT Parameters		
Volume Factor B	1	B/STB
Viscosity	11.7	cp
Total Compr. ct	3.17E-06	psi-1
Form. compr.	3.00E-06	psi-1

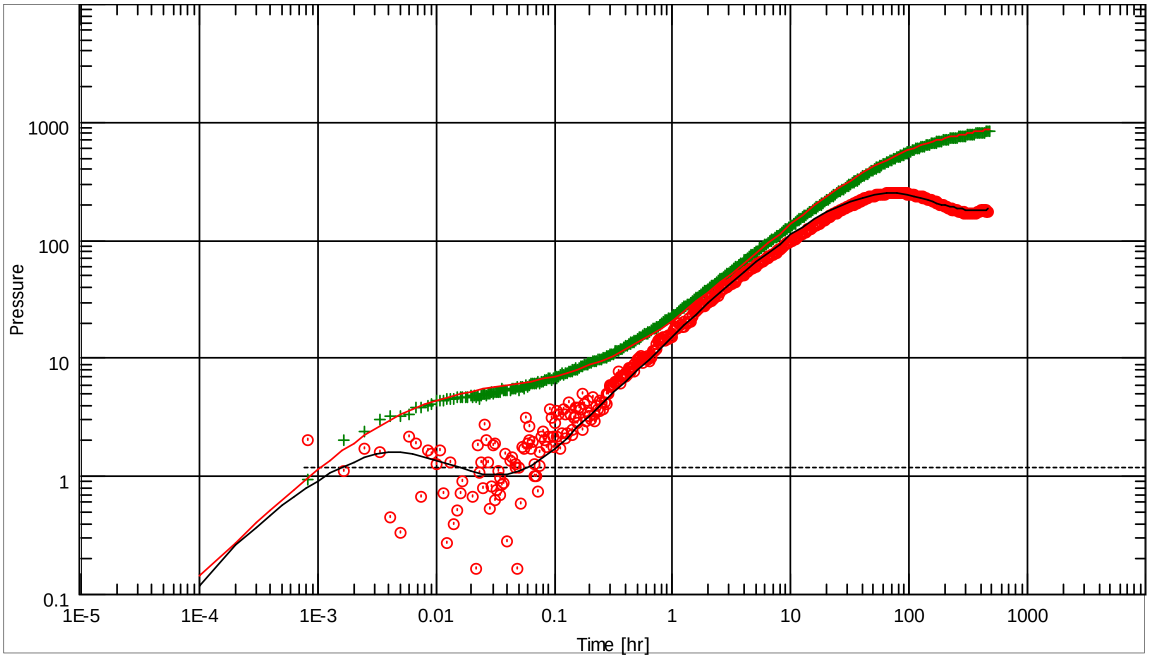

Figure 10.2: Pressure and Derivative Curve of Well TW022

Figure 10.2 shows a pressure and pressure derivative curve obtained form the analysis of pressure data from well TW022. This match was achieved with a multilayer model, but there is evidence that this well encountered 2 caverns while drilling. The result of the analysis of well TW022 above with available models from commercial software is presented in the Table 10.2.

`

Table 10.2: Results of the Analysis of Well TW022

Test Parameters		
Test Type	Standard	
Fluid Type	Oil	
Rw	0.489501	ft
h	328.084	ft
Phi	0.1	--
Selected Model		
Model Option	Multi-Layer, Commingled	
Well	Vertical	
Main Model Parameters		
TMatch	643	1/hr
PMatch	0.419	1/psia
C	0.00312	bbl/psi
Total Skin	-3.61	--
k.h, total	6810	md.ft
k, average	262	md
Pi	8574.51	psia
Model Parameters		
Layer 1		
Vertical - Homogeneous - Circle		
Skin	-3.6	--
k	521	md
h	13	ft
Phi	0.1	--
Re - No flow	380	ft
Layer 2		
Vertical - Two porosity PSS - Infinite		
Skin	-5.75	--
k	3.27	md
h	13	ft
Phi	0.1	--
Omega	0.433	
Lambda	2.24E-07	STB/D
Wellbore & other reservoir parameters		psia
Pi	8574.51	psi
C	0.00312	Fraction
PVT Parameters		
Volume Factor B	1	B/STB
Viscosity	1	cp
Total Compr. ct	3.00E-06	psi-1
Form. compr.	3.00E-06	psi-1

`

CHAPTER XI

CONCLUSIONS

Based upon work performed for this thesis the following conclusions were drawn.

1) Pressure transient testing is a reliable method for detecting and evaluating reservoir heterogeneities that affect reservoir fluid flow and reservoir performance in vuggy naturally fractured reservoirs.
2) The pressure response behavior of vuggy naturally fractured reservoirs can be match using a variety of analytical models.
3) The use of the pressure derivative curve is essential for determining a suitable model for the transient behavior.
4) Conventional models available in commercial software were not sufficient to analyze some of the more complex responses observable in this study.
5) Field examples differentiate between pressure responses obtained from a vuggy naturally fractured reservoir from that obtained from a naturally fractured reservoir without vugs.
6) Information obtained from well tests should be combined with other sources such as geological information, well logs, core sample data, production data and drilling information in order to properly characterize the well and reservoir properties.
7) The models that can be used for the analysis of vuggy naturally fractured reservoirs are summarized in the Table 11.1. The various parameters for the description of each model are provided in the table.

`

Table 11.1: Summary of Reservoir Models and Description Parameters

Model	**Parameters**	**Applications**
Homogenous	*kh* and s	Highly fractured reservoir or low permeability matrix
Radial Composite	$(kh)_1$ and $(kh)_2$ and s	Regionally fractured reservoir
Single fracture system	F_{cD}, s_f, d_f, k_f and s	Reservoir with dominant fracture
Double porosity	$(kh)_f$. s, ω and λ	Heavily fractured reservoir with sufficient matrix permeability
Triple porosity	$(kh)_f$, s, λ_{mf}, λ_{mv}, λ_{vf}, ω_f, ω_v	Highly vuggy, heavily fractured reservoir with sufficient matrix permeability

8) This study encountered transient behavior characteristic of each of these five reservoir model pressure responses. It is therefore possible for the same field to have wells that show pressure behaviors that can be attributed to different reservoir models.

9) Although homogeneous flow behavior was observed most frequently, the very low matrix porosity and permeability indicates that the reservoir must be, in reality, either homogeneously heterogeneous or heterogeneously homogeneous. The distribution of the observed reservoir models is summarized in Figure 11.1.

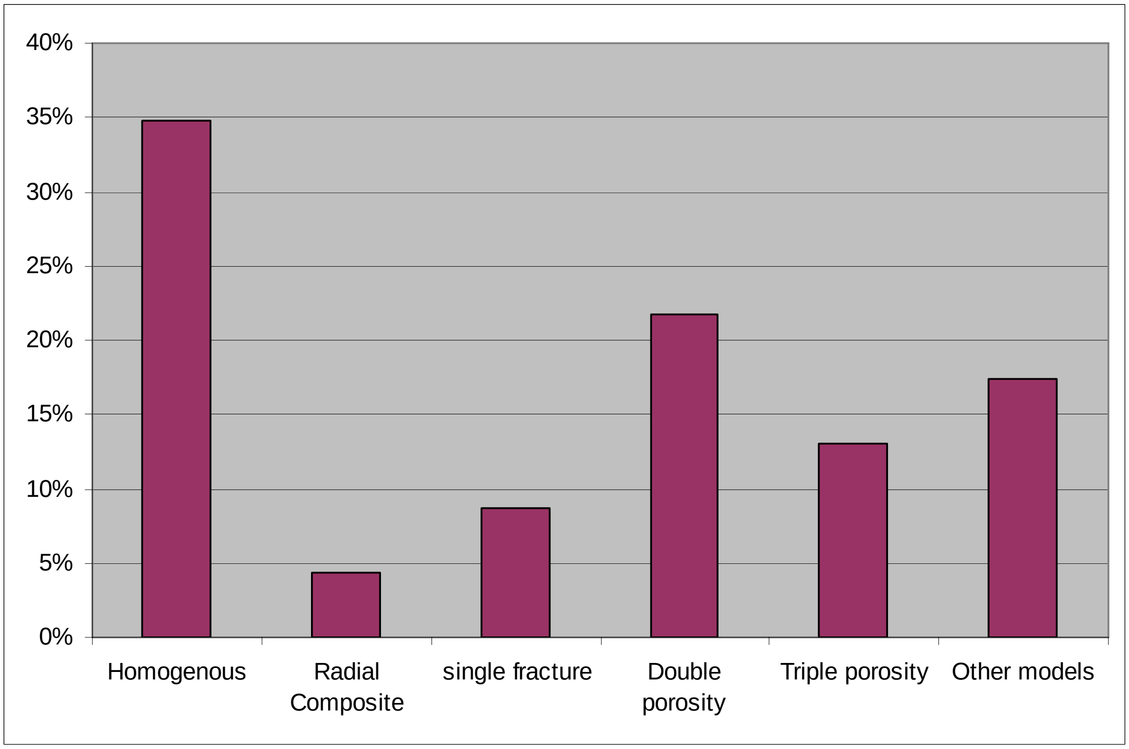

Figure 11.1: Distribution of Reservoir Models for Wells in Heterogeneous Vuggy NFR Field

10) The triple porosity model proved to be very useful in analyzing some of the pressure transient test data. Four of the wells examined exhibited triple porosity behavior.

11) With the understanding of the triple porosity behavior, it is important to reconsider the interpretation of the double porosity reservoir model analyses. First of all, the double-porosity model deals with 2 porosity systems and the valley is assumed to represent flow from the matrix to the fracture. With our understanding of the triple porosity model, it is possible for the valley observed

in the double porosity model to represent the contribution of the vug system to the fracture while the contribution from the matrix is not yet observed on the build-up test due to well test time constraints. The valley observed in the double-porosity model matches could as well be representative of the matrix contribution to the fracture while an initial valley (vug-fracture interporosity flow) may be hidden by a high wellbore storage.

NOMENCLATURE

Variables

A = cross-sectional area to flow, [ft^2]

B = gas formation volume factor, [rb/stb]

C = wellbore storage coefficient, [bbl/psi]

C_D = dimensionless wellbore storage coefficient

c_t = total system compressibility, [psia^{-1}]

c_{wb} = wellbore fluid compressibility, [psia^{-1}]

F_{CD} = dimensionless fracture conductivity [= $k_f w/kx_f$]

h = net reservoir thickness, [ft]

k = average permeability of the reservoir, [md]

k_f = fracture permeability (fracture referred to bulk volume), [md]

k_h = horizontal permeability, [md]

k_v = vertical permeability, [md]

L = Length of linear reservoir, [ft]

p = absolute pressure, [psia]

pi = initial reservoir pressure, [psia]

p_{Df} = dimensionless pressure for the fracture

p_{Dm} = dimensionless pressure for the matrix

p_{wD} = dimensionless pressure at the wellbore

`

p_{wDL} = dimensionless pressure at the wellbore for linear flow 82

p_{wf} = flowing bottomhole pressure, [psia]

p_{ws} = shut in bottomhole pressure, [psia]

q = production rate, [stb/D]

r = radius, [ft]

r_D = dimensionless radius

r_e = reservoir drainage radius, [ft]

r_{eD} = dimensionless reservoir drainage radius

r_w = wellbore radius, [ft]

r_r = radius of grid block, [ft]

s = skin factor, [dimensionless]

t = time, [days]

t_D = dimensionless time [= $0.00633kt/\varphi\mu c_t r_w^2$]

V_{wb} = wellbore volume, [ft^3]

w = width of rectangular reservoir , [ft]

w_f = width of the fracture, [ft]

x = distance to the x-direction, [ft]

x_e = distance from well to outer boundary, [ft]

x_f = fracture half-length, [ft]

`

Subscripts

D = dimensionless

f = fracture

m = matrix

e = effective

Greek Symbols

β = grid multiplier

φ = porosity, [fraction]

λ = interporosity flow parameter

μ = viscosity, [cp]

Δp = pressure change, [psia]

Δp_s = pressure change caused by skin effect, [psia]

Δt = shut in time, [days]

ω = storativity ratio

π = constant

`

REFERENCES

1. Campanella, J.D, Wadleigh, E.E and Gilman, J.R. : “Flow Characterization – Critical for Efficiency of Field Operations and IOR” paper SPE 58996 presented at SPE International Petroleum Conference and Exhibition in Mexico, 1-3 February 2000, Villahermosa, Mexico.
2. Choquette, P.W. and Pray, L.C.: “Geologic Nomenclature and Classification of Porosity in Sedimentary Carbonates,” *AAPG Bull.* (1970) **54,** No. 2, 207.
3. Nelson, R.A.: “Geologic Analysis of Naturally Fractured Reservoirs,” Gulf Professional Publishing, Woburn, Massachusetts, 2001.
4. Warren, J.E. and Root, P.J.: “The Behavior of Naturally Fractured Reservoirs,” *SPEJ* (September 1963) 245.
5. Lucia, F.J.: “Petrophysical Parameters Estimated From Visual Descriptions: A Field Classification of Carbonate Pore Space,” *JPT* (March 1983) 629.
6. Quintero, L. *et al.*: “Comparison of Permeability From NMR and Production Analysis in Carbonate Reservoirs,” paper SPE California Regional Meeting, Bakersfield, California, 27-29 March.
7. Camacho-Velazquez, R., Vasquez, M., Castrejon-Aivar, R., and Arana-Ortiz, V.: “Pressure-Transient and Decline-Curve Behavior in Naturally Fractured Vuggy Carbonate Reservoirs,” paper SPE 77689 presented at the 2002 SPE Annual Technical Conference and Exhibition, San Antonio, Texas, 29 September – 2 October.

`

8. Casar-Gonzalez, R. and Suro-Perez, V.: "Stochastic Imaging of Vuggy Formations," paper SPE 58998 presented at the 2000 SPE International Petroleum Conference and Exhibition in Mexico, Villahermosa, Mexico, 1-3 February.
9. Neale, G. H. and Nader, W, K.: "The Permeability of a Uniformly Vuggy Porous Medium," *SPEJ* (April 1973) 69.
10. Cinco-Ley, H.: "Well-Test Analysis for Naturally Fractured Reservoirs," *JPT* (Jan. 1996) 51.
11. Mavor, M.J. and Cinco-Ley, H.: "Transient Pressure Behavior of Naturally Fractures Reservoirs," paper SPE 7977 presented at the 1979 SPE California Regional Meeting, Ventura, California, 18-20 April.
12. Kazemi, H.: "Pressure Transient Analysis of Naturally Fractured Reservoirs with Uniform Fracture Distribution," *SPEJ* (December 1969) 451.
13. De Swaan O. A.: "Analytic Solutions for Determining Naturally Fractured Reservoir Properties by Well Testing," *SPEJ* (June 1976) 117.
14. Najurieta, H.L.: "A Theory for the Pressure Transient Analysis in Naturally Fractured Reservoirs," paper SPE 6017 presented at the 1976 SPE Annual Technical Conference, New Orleans, 3-6 October.
15. Bourdet, D. and Gringarten, A.C.: "Determination of Fissure Volume and Block Size in Fractured Reservoirs by Type-Curve Analysis," paper SPE 9293 presented at the 1980 Annual Fall Technical Conference and Exhibition SPE-AIME, Dallas, 21-24 September.

`

16. Gringarten, A.C., Burgess, T.M., Viturat, D., Pelissier, J., and Aubry, M.: "Evaluating Fissured Formation Geometry from Well Test Data: a Field Example," paper SPE 10182 presented at the 1981 Annual Fall Technical Conference and Exhibition SPE-AIME, San Antonio, Texas, 5-7 October.

17. Bourdet, D., Alagoa, A., Ayoub, J.A., Pirard, Y.M., and Melun, J.: "New Type Curves Aid Analysis of Fissured Zone Well Tests," *World Oil* (April 1984) 111.

18. Bourdet, D., Ayoub J., Whittle T., Pirard Y., and Kniazeff V.:"Interpreting Well Tests in Fractured Reservoirs," *World Oil* (October 1983) 77.

19. Abdassah, D. and Ershaghi, I.: "Triple-porosity Systems for Representing Naturally Fractured Reservoirs," *SPEFE* (April 1986), 113.

20. Dreier, J., Ozkan, E., and Kazemi, H.: "New Analytical Pressure-Transient Models to Detect and Characterize Reservoirs with Multiple Fracture Systems," paper SPE 92039. presented at the 2004 International Petroleum Conference, Puebla, Mexico, 8-9 November 2004.

21. Lee, W.J., Rollins, J.B., and Spivey, J.P.: *Pressure Transient Testing*, Textbook Series, SPE, Richardson, Texas (1996) **9**, 135.

22. Lee, W.J. and Wattenbarger, R.A.: *Gas Reservoir Engineering*, Textbook Series, SPE, Richardson, Texas (1996) **5**, 256.

23. Agarwal, R.G., Al-Hussainy,, R., and Ramey, H.J. Jr.: " An Investigation of Wellbore Storage and Skin Effect in Unsteady Liquid Flow – 1. Analytical Treatment," *SPEJ* (September 1970) 279; *Trans.,* AIME **249.**

`

24. Gringarten, A.C. *et al.*: "A Comparison Between Different Skin and Wellbore Storage type-Curves for Early time Transient Analysis," paper SPE 8205 presented at the 1979 SPE Annual Technical Conference and Exhibition, Las Vegas, Nevada, 23-26 September.
25. Ehlig-Economides, C.; *PETE 648: Pressure Transient Analysis*, Texas A&M University, College Station (2006).
26. Cinco-Ley, H., Samaniego V.F., and Dominguez, A.N.: "Unsteady-State Flow Behavior for a Well near a Natural Fracture," paper SPE 6019 presented at the 1976 SPE Annual Technical Conference and Exhibition, New Orleans, 3-6 October.
27. Abbaszadeh, M.D, and Cinco-Ley, H.: "Pressure Transient Behavior in a Reservoir with a Finite Conductivity Fault," *SPEFE* (March 1995) 26.

`

VITA

Name: Babatunde Tolulope Ajayi

Permanent Address: Plot 54, Road 14, Admiralty Way
Lekki, Lagos State
NIGERIA

Education: B.S., Chemical Engineering
Bosphorus University, Istanbul
Turkey, 2005

M.S., Petroleum Engineering
Texas A&M University, Petroleum Engineering Department,
College Station, Texas, U.S.A., 2007

`